Fall 12-20-2013

Predicting Voltage Abnormality Using Power System Dynamics

Nagendrakumar Beeravolu
nbeeravo@uno.edu

Predicting Voltage Abnormality Using Power System Dynamics

A Dissertation

Submitted to the Graduate Faculty of the
University of New Orleans
in partial fulfillment of the
requirements for the degree of

Doctor of Philosophy
In
Engineering and Applied Sciences
Electrical Engineering

By

Nagendrakumar Beeravolu

MS, University of New Orleans, 2010
B. Tech. JNTU, 2007

December, 2013

Acknowledgements

This dissertation would not have been possible without the guidance and the help of several individuals who in one way or another contributed and extended their valuable assistance in the preparation and completion of this study.

First I wish to express my utmost gratitude to my advisor Prof. Dr. Parviz Rastgoufard who was abundantly helpful and offered invaluable assistance, support and guidance to finish this dissertation. My association with him for over six years was a rewarding experience. I am really thankful to the members of the supervisory committee Dr. Ittiphong Leevongwat, Dr. Edit Bourgeois, Dr. Bhaskar Kura, and Dr. George Ioup for their great support throughout my masters to finish this study. I would like to thank Entergy-UNO Power and Research Laboratory for providing appropriate tools to finish this task.

Last, I would like to acknowledge and thank my parents, my sister and all of my friends for their encouragement and moral support to finish this task.

Table of Contents

List of Figures

List of Tables

Abstract

The purpose of this dissertation is to analyze dynamic behavior of a stressed power system and to correlate the dynamic responses to a near future system voltage abnormality. It is postulated that the dynamic response of a stressed power system in a short period of time-in seconds-contains sufficient information that will allow prediction of voltage abnormality in future time-in minutes. The PSSE dynamics simulator is used to study the dynamics of the IEEE 39 Bus equivalent test system. To correlate dynamic behavior to system voltage abnormality, this research utilizes two different pattern recognition methods one being algorithmic method known as Regularized Least Square Classification (RLSC) pattern recognition and the other being a statistical method known as Classification and Regression Tree (CART). Dynamics of a stressed test system is captured by introducing numerous contingencies, by driving the system to the point of abnormal operation, and by identifying those simulated contingencies that cause system voltage abnormality.

Normal and abnormal voltage cases are simulated using the PSSE dynamics tool. The results of simulation from PSSE dynamics will be divided into two sets of training and testing set data. Each of the two sets of data includes both normal and abnormal voltage cases that are used for development and validation of a discriminator. This research uses stressed system simulation results to train two RLSC and CART pattern recognition models using the training set obtained from the dynamic simulation data. After the training phase, the trained pattern recognition algorithm will be validated using the remainder of data obtained from simulation of the stressed system. This process will determine the prominent features and parameters in the process of classification of normal and abnormal voltage cases from dynamic simulation data.

Each of the algorithmic or statistical pattern recognition methods have their advantages and disadvantages and it is the intention of this dissertation to use them only to find correlations between the dynamic behavior of a stressed system in response to severe contingencies and the outcome of the system behavior in a few minutes into the future.

Key Words: Pattern recognition; Power system dynamic response; Blackouts; Voltage stability; Voltage collapse

Chapter 1

1 Introduction

1.1 Power System Stability

Security of power systems operation is gaining ever increasing importance as the system operates closer to its thermal and stability limits. Power system stability can be defined as:

- *Is the ability of an electric power system, for a given initial operating condition, to regain a state of operating equilibrium after being subjected to a physical disturbance, with most system variables bounded so that practically the entire system remains intact.*

Power system stability, the most important index in power system operation- may be categorized under two general classes relating to the voltage stability and to the angle stability driven by different forces in the system. Voltage stability is principally load driven and focuses on determining the proximity of bus voltage magnitudes to pre-determined and acceptable voltage magnitudes. Angle stability is principally generator driven focuses on the investigation of voltage angles as the balance between supply and demand changes due to occurrence of faults or disturbances in the system and this affects voltage magnitudes as well. Voltage stability is a slowly varying phenomena in seconds or minutes while angle stability is relatively faster in milli seconds and deals with systems dynamics described mathematically by differential equations of generators in the system.

Power system stability can be classified in to the two different categories of voltage and angle stability on the basis of [**1**]

- The physical nature of resulting mode of instability
- The size of the disturbance
- The devices, process and time span
- The most appropriate method of calculation and prediction of stability

Classification of power system stability on the basis of the criteria mentioned above is presented in Figure 1.1. Since the classification is based on a number of diverse conditions, it is difficult to select clearly distinct categories and to provide definitions that are rigorous and yet convenient for practical use. Classification of power system stability is an effective and convenient means to deal with the complexities of the problem, but one has to keep in mind that the overall system stability is not affected and solutions to stability problems of one category should not be at the expense of another.

This research will concentrate on voltage stability issues. The purpose of this dissertation is to analyze dynamic behavior of a stressed power system and to correlate the dynamic responses to a near future system voltage abnormality. The main goal of this dissertation is to analyze dynamic behavior of a stressed power system and to correlate the dynamic responses to a near future system voltage abnormality in order to provide the operators a lead time for remedial action and possible prevention of blackouts.

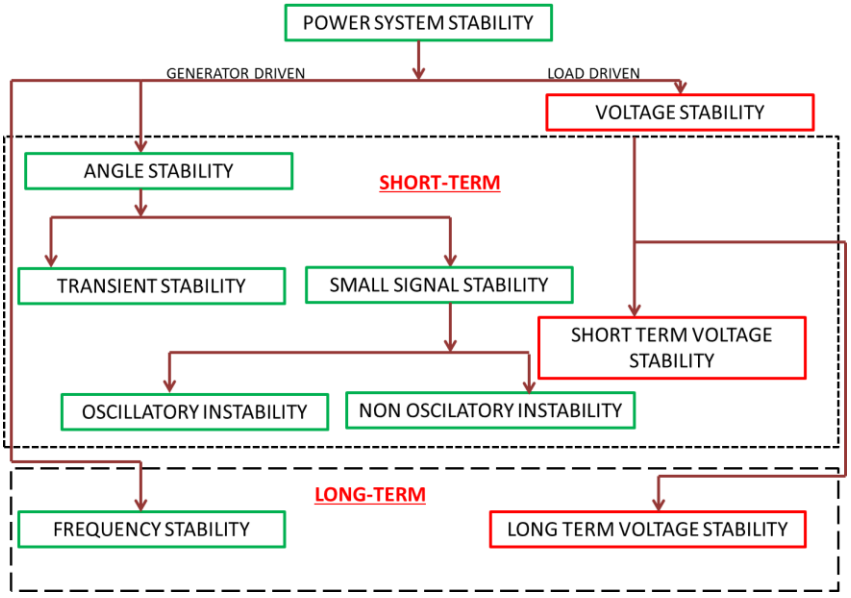

Figure 1.1: Classification of Power System Stability

As this section has provided a basic idea of power system stability and the classification of the stabilities in power systems, the next sections will cover the basics of voltage stability and a review of the voltage stability analysis methods relevant to the main objective of this dissertation.

1.2 A Review of Voltage Stability

Voltage stability can be defined as:

- *A power system at any given state and subjected to a given disturbance is voltage stable if the voltage near load buses approach post-disturbance equilibrium values. Where the disturbed state is within the region of attraction of the stable post-disturbance equilibrium. Voltage instability of a power system is its inability to maintain the steady state voltage after a disturbance in the system.* [**2**]

Voltage instability problems are more frequent on heavily stressed systems. After a system disturbance, the consequence of voltage collapse may be influenced by a variety of factors such as the strength of the transmission network, generator reactive power and voltage control limits, load characteristics, characteristics of reactive compensation devices, and action of voltage control device such as tap changing transformers.

A possible outcome of voltage instability is the loss of load or load shedding in an area where the voltage is more degraded compared to the voltage in other areas of the system. The main factor contributing to voltage instability in an area is an increase in voltage drop when resulting from active and reactive power flow through the transmission line compared to initial conditions. There is another possibility that an increase in rotor angles of generators will also cause greater system voltage drop and result in voltage instability.

Voltage instability or voltage collapse in a power system is normally perceived as slowly varying phenomena and it could be caused by variety of system dynamics. The mechanism leading to voltage collapse normally starts as the voltage decreases in an area due to the increase in load demand. The system steady state conditions change slowly initiating the voltage stabilizing elements such as load tap changers, voltage regulators, and static and dynamic compensators to respond, and correct the system changes. If these elements while stabilizing the system exceed their operating limits, they will be removed from system operation. This may prevent correction and system will degrade instead to a more severe operating condition, closer to the point of voltage collapse, and eventually to operating conditions that are uncontrollable. Because of interaction of these components and due to different dynamic time responses of these equipment, voltage collapse may take anywhere from fraction of second to tens of minutes. Due

to variation in time responses, appropriate mathematical models that capture dynamics in almost real-time to steady state models may be required to predict proximity and occurrence of voltage collapse in real-size power systems. The main reason for voltage collapse is when transmission lines are operating very close to their thermal limits and then are forced to transmit more power or when the power system has insufficient reactive power for transmission to an area with increasing load requirements.

In large scale systems, voltage collapse includes voltage magnitude and angle under heavy loading conditions. In some situations, it is hard to decouple the angle and magnitude instability from each other.

Two types of system analysis are possible; static system and dynamic system analysis [**1**]. Each approach has its appropriate use for specific system conditions and each bears its own advantages and disadvantages which will be addressed in this research. The design and analysis of accurate methods to evaluate the voltage stability of a power system and to predict incipient voltage instabilities are therefore of special interest in the field of power systems. Dynamic analyses provide the most accurate indication of the time response of the system and are useful for predicting fast occurring voltage collapses in the system but these will not provide much information about sensitivity or degree of stability. On the other hand static analyses that are based on performing system-wide sensitivity will provide the information necessary for concluding degree of instability. Static analyses involve computation of algebraic equations rather than the solution of differential equations, and hence, are much faster to compute compared to dynamic analysis for both on-line and off-line studies. However static analysis is limited because it cannot investigate the dynamic reasons for voltage instability that may be

embedded in the energy content of the system only a few seconds after occurrence of a system disturbance and long before the ultimate result of system voltage collapse.

This section has provided a brief introduction to voltage stability of a power system including static and dynamic analysis of voltage stability, along with their advantages and disadvantages. The upcoming sections of this chapter will provide a historical review of both of the voltage stability analysis methods and will also outline our approach to using these models for the prediction of patterns that may be detectible a few seconds after disturbances have occurred.

1.3 Review of Static Analysis Methods of Voltage Stability

There is several research publications ranging from papers to books related to the static analysis of voltage stability. Most of these publications document approaches that are based on using the system's Jacobian matrix and identification of singularities. The singularities of the Jacobian matrix provide a guide to the point of system voltage collapse.

Static approaches capture snapshots of system conditions at various time frames and can determine the overall stability of the system or proximity and margin to becoming unstable at that particular time frame [**1**]. A variety of tools like multiple load flow solutions [**3**], load flow feasibility [**4**], optimal power flow [**5**], steady state stability [**6**], modal analysis [**2**] [**7**] [**8**] [**9**] [**10**] [**11**], the P-V curve, Q-V curve, Eigen value, singular value of Jacobian matrix [**12**] [**13**] , sensitivity and energy based methods have been proposed on static analysis of voltage stability

[**1**] [**14**] [**15**] [**16**] [**17**] [**18**] [**19**]. This section will only provide the methodology of each of these static analysis methods. Chapter 3 of this dissertation report will elaborate on these methods.

In the past, all the utilities depended on conventional power flow programs for static analysis and the voltage stability by computing P-V and V-Q curves at different buses in the system while the load at these buses are increased. This method of static analysis is a time consuming process because it has to undergo a large number of power flow solutions involving several studies for each bus in the system. Also, the resulting P-V and V-Q curves will not provide much information about the cause of instability since they are mainly concentrated on individual buses in the power system network. There are some approaches such as V-Q sensitivity modal analysis which provide more information regarding voltage stability [**1**].

V-Q sensitivity analysis which is used in modal analysis, is a good measure for the sensitivity of a system [**1**]. This will use the same conventional power flow model and system Jacobian matrix. Generally system voltage stability is affected by P and Q. For V-Q sensitivity analysis, P is kept constant and the voltage stability is determined by considering incremental relationship between Q and V. When P is kept constant the Jacobian matrix transforms to a reduced Jacobian matrix. The inverse of this matrix becomes the reduced V-Q Jacobian matrix where the i^{th} diagonal element of the matrix is the V-Q sensitivity of the i^{th} bus. A positive V-Q sensitivity represents a stable operation. The smaller value of sensitivity implies a more stable system so as the sensitivity value increases stability decreases. A negative value for V-Q sensitivity represents unstable operation.

J. Bian [**20**] compared various methods for studying voltage stability and proposed [**21**] to use the smallest Eigen values λ_{min} of the Jacobian matrix to measure voltage stability level of a

system. The smallest Eigen value is defined as the voltage stability margin and the singularity of the Jacobian matrix, reflected by $\lambda_{min}=0$, serves as the voltage instability indicator.

G.K. Morison, B. Gao, P. Kundar proposed a method referred to as V-Q modal analysis [**11**] . This method is based on using the reduced Jacobian matrix formed in V-Q sensitivity analysis to provide proximity of the system to voltage instability as well as the main contributing factor for it. In this method, a smaller number of Eigen values are calculated from the reduced Jacobian matrix which maintains the Q-V relationship of the network and also includes the characteristics of generators, loads, reactive power compensating devices, and HVDC converters. The Eigen values of reduced Jacobian matrix will identify different modes of the system which will lead to voltage instability. The magnitude of the Eigen value provides a relative measure of proximity to voltage instability. If the magnitude of modal Eigen value is equal to zero, then the corresponding modal voltage collapses. Left and right Eigen vectors of critical modes will provide the information concerning the mechanism for the voltage collapse by identifying the elements that participate in the ultimate voltage collapse in the system. For this purpose, they propose a concept called bus participation factor. Branches with large participation factors to the critical mode will consume more reactive power for incremental change in reactive power and will lead to the voltage instability.

S. Chandrabhan and G. Marcus have developed a PC-based MATLAB prototype application [**22**] to analyze the voltage stability of a power network using the same modal analysis proposed in [**11**] and some additional techniques like power flow analysis, V-P/V-Q curves.

Modal analysis has some disadvantages [**23**] in requiring the Jacobian matrix to be a square matrix, suitable for analyzing only PQ bus reactive power control where the active power is considered as zero, and assumes constant voltages by not considering generator AVR at PV buses.

C. Li-jun and E. Istavan [**23**] present their work by considering static voltage stability analysis by the use of a singular value approach for both active and reactive power control. They applied feasible controls as input signals and the voltage magnitude of critical buses as output signals and developed a MIMO (multi input and multi output) transfer function of multi-machine system and singular value decomposition (SVD) to identify the maximum and minimum singular values of the transfer function matrix . The authors propose to monitor the maximum input and output vectors and to relate the change to the input that has the largest influence on the corresponding output and the buses where the voltage magnitude is critical.

Static analysis for voltage stability methods are easier to implement compared to dynamic analysis methods because the modeling of loads and generators is relatively simple and requires less computing time in the simulation. However these methods are not as accurate because of the simplistic models.

This section has provided a review on static voltage stability analysis by introducing the work performed by different researchers around the globe and provides a brief introduction to the use of static voltage stability analysis methods. A review of dynamic stability analysis and a review on large scale blackouts occurred will be presented in the next sections of this chapter.

1.4 Review of Dynamic Analysis Methods of Voltage Stability

A power system is typical a large dynamic system and its dynamic behavior has great influence on the voltage stability. There are several ongoing research efforts related to the study of dynamic voltage stability of power system to prevent the voltage collapse in the power system subsequent blackouts.

In the dynamical analysis, voltage stability can be classified into short term, midterm and long term dynamics based on the time scale of operation. By the name itself, short term dynamics correspond to fast acting devices like generators and induction motors. Midterm and long term dynamics correspond to slow acting devices like transformer load tap changers, generator excitation limiters and generator automatic voltage regulators [**2**].

G. K. Morison, B. Gao, P. Kundar in [**16**] have shown how voltage instability can occur and the situations in which the modeling of loads, load tap changers and generator maximum excitation limiters will impact the system voltage stability. Reference [**24**] [**25**] investigated the dynamic nature of voltage instability considering dynamic load modeling effect on the accuracy of voltage stability analysis. To study dynamic voltage stability of a system, one needs to consider the dynamic model for all the elements in the power system [**26**] and capture all the dynamics of different elements in the system to find out the exact reason for voltage collapse. In reference [**27**] voltage instability is associated with tap-changing transformer dynamics by defining the voltage stability region in terms of allowable transformer settings. In reference [**28**] the methods have employed a nonlinear dynamic model of OLTC, impedance loads and decoupled reactive power voltage relations to reconstruct the voltage collapse phenomenon and developed a method to construct stability regions. In reference [**29**], the authors analyzed

dynamic phenomenon of voltage collapse by dynamic simulations using induction motor models, the paper explains how voltage collapse starts locally at the weakest node and eventually spreads out to the other weak nodes.

K. Sun, S. Likathe, V. Vittal, V. S. Kolluri, S. Mandal [**30**] have proposed an online dynamic security assessment scheme for large scale power systems using Phasor Measurement Units (PMU) data and Decision Trees (DTs). This scheme will provide the dynamic security of the power system from the available PMU real-time measurements and the DTs predictors including fault type and location, bus voltage angles, MW transfers across lines or interfaces, and generator output.

Cat S. M. Wong, P. Rastgoufard, and D. Mader in reference [**31**] used real time simulation computing facilities to determine and detect signs and patterns of power system dynamic behaviors to predict voltage stability.

The purpose of this dissertation is to analyze dynamic behavior of a stressed power system and to correlate the dynamic responses to the future system voltage abnormality. The software package PSSE Dynamics simulator is used to study the dynamics of the IEEE 39 Bus equivalent test system. To correlate dynamic behavior to system voltage abnormality, this dissertation utilizes pattern recognition methods including algorithmic Regularized Least Square Classification (RLSC) method and the statistical Classification and Regression Tree (CART) method.

This section has provided a review of the research performed using the dynamic analysis for the voltage stability detection. The next section of this chapter will review the major

blackouts reported during the past and the reason behind the system voltage collapse will be discussed.

1.5 Historical Review of Major Blackouts

There are several major power system blackouts that have occurred in last half century. All the published reports on blackouts stated that even though each system was designed for N-1 contingencies, it was still not enough to secure stable system operations. An IEEE task force report on "Blackout experiences and Lessons, Best Practices for System Dynamic Performance, and the Role of New Technologies" [**32**] has reported on the major blackouts that have occurred around the globe with the reasons behind the blackouts, and offered the best practices needed to improve the dynamic performance of the system to avoid blackouts. The following are summaries of some of the major blackout events that were reported.

The first major blackout reported was on November 9th 1965 in the United States northeast area [**33**] [**34**]. Because of heavy loading conditions one of the five transmission lines was tripped by a backup relay low load level settings. This resulted in tripping the remaining four transmission lines causing 1700MW of load to be diverted to other lines there by over loading them which resulted in voltage collapse. This blackout effected 30 million people and New York City was in darkness for 13 hours. A special issue [**35**] published in 2005 talks about changes made in power technology and policy after forty years from blackout occurred in 1965.

The next major blackout occurred on July 13th 1977 in the US [**33**] because of collapse in the Con Edison System. A thunderstorm lightning strike hit two transmission lines and a protective equipment malfunction tripped three out of four transmission lines. This situation

overloaded all the remaining transmission lines for 35 minutes causing them to trip. After 6 minutes the whole system was out of operation. This blackout left 8 million people in darkness including New York City and took 5 to 25 hours to restore the system.

A decade later on July 23rd 1987 a major blackout occurred in Tokyo, Japan [**33**]. This blackout occurred because of high peak demand due to extreme hot weather conditions. The increased demand gradually reduced the voltage of the 500kV system to 460kV in five minutes. The constant power characteristic loads such as air conditioning systems gradually reduced the voltage and caused dynamic voltage collapse. The Tokyo blackout affected 2.8 million customers with 3.8GW of load lost. The whole system was recovered relatively fast in 90 minutes after the voltage collapse.

The blackout on July 2nd 1996 in the Western North American power system [**33**] was due to a short circuit of a 1300km series compensated 345kV transmission line caused by flashover to a tree. This blackout affected 2 million people with 11,850MW of load loss.

The US-Canadian Blackout on August 14th 2003 [**33**] [**36**] was initiated by a 345kV transmission line tripping due to a tree contact. Another line subsequently over loaded, sagged and touched a tree after the first line was disconnected. At the same time, the supervisory control and data acquisition (SCADA) system designed to warn operators was not functioning properly. Several transmission lines reversed their power flow eventually causing a cascading blackout of entire region. During this voltage collapse, 400 transmission lines and 531 generating units at 261 power plants tripped. This blackout affected 50 million people with 63GW of load interruption.

The European blackout occurred on November 4th 2006 [**37**] in the UCTE (Union for the Coordination of the Transmission of Electricity) interconnected power grid which coordinates 34 transmission system operators in 23 European countries. This blackout started with a 380kV transmission line tripping. This blackout affected 15 million people in Europe with 14.5 GW of load interrupted in more than 10 countries.

The Arizona-Southern California outage occurred on September 8th 2011 [**38**] in United States of America. An 11-minute system disturbance in the Pacific Southwest lead to cascading outages and left approximately 2.7 million customers without power.

This section has reviewed the past major blackouts reported around the world. The next section of this chapter will concentrate on the main purpose of this dissertation and explain the methodology used in predicting voltage collapse.

1.6 Scope

This research continues the previous research completed at Tulane University by S. M. Wong and P. Rastgoufard on "Unification of Angle and Magnitude Stability to Investigate Voltage Stability of Large-Scale Power System" [**31**] [**39**] [**40**] [**41**], and at the University of New Orleans by N Beeravolu and P. Rastgoufard on "Pattern Recognition of Power Systems Voltage Stability Using Real Time Simulations" [**42**].

The purpose of this dissertation is to analyze dynamic behavior of a stressed power system and to correlate the dynamic responses to the future system voltage abnormality. It is postulated that the dynamic response of a stressed power system in a short period of time-in seconds contains sufficient information that will allow prediction of voltage abnormality in

future time-in minutes [**40**] [**42**]. The PSSE Dynamics simulator software package was used to study the dynamics of the IEEE 39 Bus equivalent test system. To correlate dynamic behavior to system voltage abnormality, this research utilizes two pattern recognition methods including the algorithmic Regularized Least Square Classification (RLSC) method and the statistical Classification and Regression Tree (CART) method.

Normal and abnormal voltage cases are simulated using the PSSE Dynamics tool and the results of the simulation from PSSE Dynamics will be divided into two sets of training and testing data. Each of the two sets of data includes both normal and abnormal voltage cases that are used for development and validation of a discriminator. This research uses stressed system simulation results to train the RLSC and CART pattern recognition models using the training set obtained from the dynamic simulation data. After the training phase, the trained pattern recognition algorithm will be validated using the remainder of data obtained from simulation of the stressed system. This process will determine the prominent features and parameters in the process of classification of normal and abnormal voltage cases from dynamic simulation data.

The reminder of this dissertation discusses traditional methods for determining voltage stability in Chapter 2, dissertation objectives and outline of methodology in Chapter 3, modeling of the test system in Chapter 4, with results and voltage stability prediction analysis on the test system in Chapter 5, Chapter 6 concludes with the summary of this dissertation and discusses future work concerning the application of the proposed method.

This dissertation now proceeds to outline the tradition methods of determining voltage stability of power systems in Chapter 2.

Chapter 2

2 Methods of Voltage Stability Analysis

Chapter 1 of this dissertation has already provided some idea about the voltage stability phenomenon. Voltage stability mainly deals with loads and voltage magnitudes. This chapter discusses about traditional methods to determine the voltage stability.

As mentioned in Chapter 1, two types of system analysis are possible for voltage stability studies; static system analysis and dynamic system analysis. Each approach may be used as appropriate for specific system conditions. Each bears its own advantages and disadvantages which we shall addressed in this research. Design and analysis of accurate methods to evaluate the voltage stability of a power system and predicting incipient voltage instabilities are therefore of special interest in the field of power systems. Dynamic analyses provide the most accurate indication of the time response of the system and are useful for predicting fast occurring voltage collapses in the system, however these studies will not provide much information about sensitivity or degree of stability. On the other hand, static analyses that are based on performing system-wide sensitivity studies will provide the information necessary for determining the degree of instability for a system. Static analysis involves the computation of algebraic equations rather than the solution of differential equations. Consequently it is much faster compared to dynamic analysis for both on-line and off-line studies. That said, static analysis cannot investigate the dynamic reasons for voltage instability that may be embedded in the energy content of the system only a few seconds after occurrence of a system disturbance and long before the ultimate result of system voltage collapse. This dissertation will outline the approach

in using static and dynamic system models for the prediction of patterns that may be detectible a few seconds after disturbances to predict system voltage instabilities.

2.1 Static Voltage Stability Analysis methods

Static analysis for voltage stability captures snapshots of system conditions with various time frames along the time-domain trajectory. The time derivatives of all the state variables are assumed to be zero, so that the overall system equations are reduced to purely algebraic equations. This dissertation will cover some of the traditional static voltage stability analyses in the following sub-sections.

2.1.1 P-V Curve Analysis

P-V curve analysis is used to determine voltage stability of a radial system and also a large meshed network. For this analysis P, i.e. power at a particular area, is increased in steps and the resulting voltage V is observed at some critical load buses. Curves for those particular buses will be plotted to determine the voltage stability of a system by a static analysis approach. The main disadvantage of this method is that the power flow solution will diverge at the nose or maximum power capability of the curve and the generation capability needs to be rescheduled as the load increases.

To explain the P-V curve analysis let us assume a simple circuit which has a single generator, single transmission line and a load. This circuit consists of two buses. The one line diagram for this circuit is shown in Figure 2.1.

P-V curves are useful in deriving how much load shedding should be done to establish pre-fault network conditions even with the maximum increase of reactive power supply from various automatic switching of capacitors or condensers.

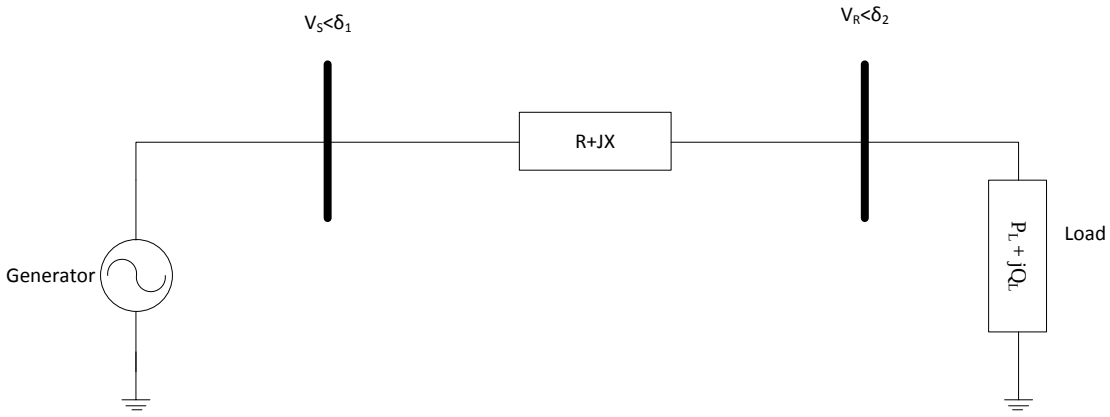

Figure 2.1: A two-bus test system

Here the complex load assumed is $S_L = P_L + jQ_L$, where P_L and Q_L real and reactive power loads respectively. V_R is the receiving end voltage and V_S is the sending end voltage. R and X are the respective resistance and reactance of the transmission line. CosΦ is the load power factor. The complex load power can be written as Equation (2.1).

$$S_L = |V_R|I^* = |V_R||I|(\cos\Phi + i\ \sin\Phi) = |V_R||I|e^{i\Phi} \qquad (2.1)$$

Let us consider $\beta = \tan\Phi$. Equation (2.1) can be written as Equation (2.2).

$$S_L = P_L(1 + i\beta) = Q_L\left(\frac{1}{\beta} + i\right) \qquad (2.2)$$

From equation (2.1), P_L and Q_L can be written as Equation (2.3) and Equation (2.4).

$$P_L = |V_R||I|\cos\Phi \qquad (2.3)$$

$$Q_L = |V_R||I|\sin\Phi \qquad (2.4)$$

The network equations for the circuit considered for the case where resistance of transmission line assumed as zero are given in Equation (2.5).

$$P_L = \frac{|V_S||V_R|}{X} \sin \delta_{12} \tag{2.5}$$

$$Q_L = -\frac{|V_S|^2}{X} + \frac{|V_S||V_R|}{X} \cos \delta_{12} \tag{2.6}$$

Where $\delta_{12} = \angle\delta_1 \text{-} \angle\delta_2$ is the bus voltages angle difference.

$$\frac{|V_S||V_R|}{X} \cos \delta_{12} = Q_L + \frac{|V_S|^2}{X} \tag{2.7}$$

Applying trigonometric identities on Equations (2.6) and (2.7) will produce Equation (2.8).

$$P_L^2 + \left[\beta P_L + \frac{|V_S|^2}{X}\right]^2 = \frac{|V_S|^2 |V_R|^2}{X^2} \tag{2.8}$$

Solving Equation (2.8) for V_R will give Equation (2.9).

$$|V_R|^2 = \frac{|V_S|^2}{2} - \beta P_L X \pm \left[\frac{|V_S|^4}{4} - P_L X (P_L X + |V_S|^2 \beta)\right]^{\frac{1}{2}} \tag{2.9}$$

The Equation (2.9) can give P-V curve when the values of V_S , β, and X are fixed. As P real power load changes, two voltage solutions will result at each loading case. At P=Pmax, the voltage solutions will be of the same value and this voltage is called the critical voltage. If P is increased beyond Pmax, then the solution will become unsolvable indicating voltage collapse. The P-V curves for $V_1 = 1\angle 0$, X=0.4 p.u and for different power factor are shown in Figure 2.2.

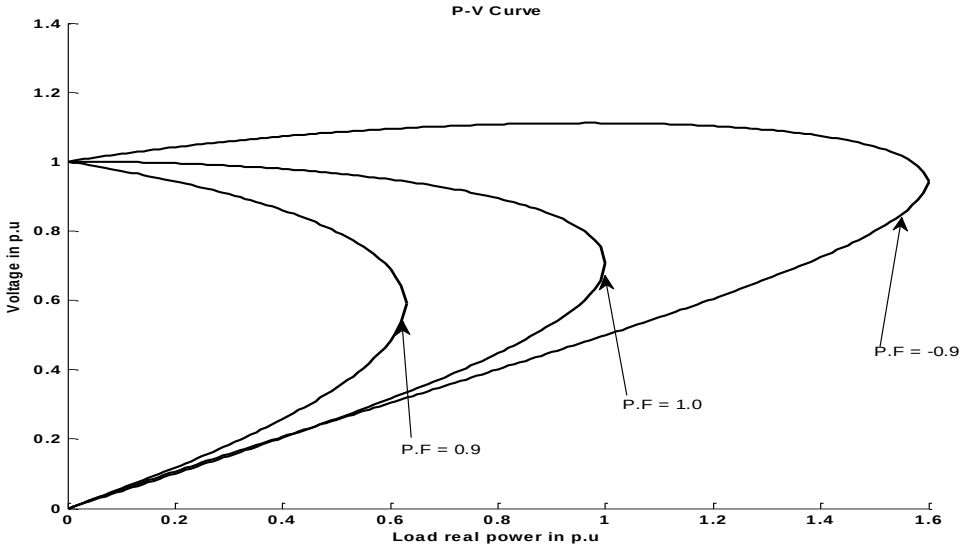

Figure 2.2: P-V Curve

2.1.2 V-Q Curve Analysis

V-Q curves plot voltage at a test or critical bus versus reactive power on the same bus. V-Q curves will provide good insight in to system reactive power capabilities under both normal and contingency conditions. The V-Q curves have many advantages. V-Q curves will show reactive power margin at a test bus. Reactive power compensation will provide security to voltage stability problems. This is determined by plotting reactive power compensations onto the V-Q curves. The slope of the V-Q curve will indicate stiffness of the test bus. It should be noted however that this method artificially stresses a single bus and should be confirmed by more realistic methods before reaching a conclusion.

2.1.3 V-Q Sensitivity Analysis

The V-Q sensitivity analysis will provide information regarding the sensitivity of a bus voltage with respect to the reactive power consumption. This analysis can provide system wide

voltage stability related information and can also identify areas that have potential problems. The linearized steady state power systems equations can be expressed as Equation (2.10).

$$\begin{bmatrix} \underline{\Delta P} \\ \underline{\Delta Q} \end{bmatrix} = \begin{bmatrix} \underline{J_{P\theta}} & \underline{J_{PV}} \\ \underline{J_{Q\theta}} & \underline{J_{QV}} \end{bmatrix} \begin{bmatrix} \underline{\Delta\theta} \\ \underline{\Delta V} \end{bmatrix} \qquad (2.10)$$

Where $\underline{\Delta P}$= vector of incremental change in bus real powers

$\underline{\Delta Q}$= vector of incremental change in bus reactive power injections

$\underline{\Delta V}$= vector of incremental change in bus voltage magnitude

$\underline{\Delta\theta}$= vector of incremental change in bus voltage angle

Here the elements of the Jacobian matrix J will give the sensitivity between power flow (Real power P, Reactive power Q) and voltage (Bus Voltage Magnitude V and Angle θ) changes.

The general structure of the system model for voltage stability analysis is similar to that of transient stability analysis. The overall system equations, comprising a set of first-order differential equations can be mathematically expressed as Equation (2.11).

$$\dot{\underline{X}} = \underline{f}(\underline{X}, \underline{V}) \qquad (2.11)$$

In Equation (2.11) $\underline{X}$ and $\underline{V}$ represent the state vector and bus voltage vector respectively.

Rewriting the linear relationship between power and voltage for each device when $\dot{X}$=0 for equation (2.10) can be expressed as Equation (2.12).

$$\begin{bmatrix} \underline{\Delta P_d} \\ \underline{\Delta Q_d} \end{bmatrix} = \begin{bmatrix} \underline{A_{11}} & \underline{A_{12}} \\ \underline{A_{21}} & \underline{A_{22}} \end{bmatrix} \begin{bmatrix} \underline{\Delta \theta_d} \\ \underline{\Delta V_d} \end{bmatrix} \quad (2.12)$$

Here "d" stands for device.

All the above elements are for a particular device. $\underline{A_{11}}$, $\underline{A_{12}}$, $\underline{A_{21}}$ and $\underline{A_{22}}$ matrices will represent system Jacobian elements.

V-Q sensitivity analysis is done by keeping the real power P constant and evaluating voltage stability by considering the incremental relationship between Q and V. when $\underline{\Delta P}$=0 we can derive Equation (2.13) from equation (2.10)

$$\underline{\Delta Q} = \underline{J_R}\underline{\Delta V} \quad (2.13)$$

Where

$$\underline{J_R} = \left[\underline{J_{QV}} - \underline{J_{Q\theta}}\underline{J_{P\theta}^{-1}}\underline{J_{PV}}\right] \quad (2.14)$$

$\underline{J_R}$ is called as reduced Jacobian matrix of the system Equation 2.13 can also be written as equation (2.15)

$$\underline{\Delta V} = \underline{J_R^{-1}}\underline{\Delta Q} \quad (2.15)$$

Where $\underline{J_R}^{-1}$ is the inverse of the reduced V-Q Jacobian and its 'i^{th}' diagonal element will provide V-Q sensitivity at bus 'I'.

As previously mentioned, V-Q sensitivity at a bus is the slope of Q-V curve at given operating conditions. A positive V-Q sensitivity indicates a stable condition and negative indicates an unstable condition. Because of the nonlinear nature of the V-Q relationship, the

magnitudes of the sensitivities for different system conditions do not provide a direct measure of the relative degree of stability.

2.1.4 Q-V Modal Analysis

Eigen values and Eigen vectors of reduced Jacobian matrix $\underline{J_R}$ will be useful in describing voltage stability characteristics.

Let us consider $\underline{J_R} = \underline{R}\,\underline{\Lambda}\,\underline{L}$ (2.16)

Where $\underline{R}$= right Eigen vector matrix of $\underline{J_R}$

$\underline{L}$= left Eigen vector matrix of $\underline{J_R}$

$\underline{\Lambda}$=Diagonal Eigen value matrix of $\underline{J_R}$

Using modal transformation Equation (2.16) can be written as Equation (2.17).

$$\underline{J_R^{-1}} = \underline{R\Lambda^{-1}L} \tag{2.17}$$

Substituting Equation (2.17) in to Equation (2.13) will give Equation (2.18)

$$\underline{\Delta V} = \underline{R\Lambda^{-1}L}\,\underline{\Delta Q} \tag{2.18}$$

$$\underline{\Delta V} = \sum_i \frac{r_i l_i}{\lambda_i}\,\underline{\Delta Q} \tag{2.19}$$

Here 'r_i' is the 'i^{th}' column right Eigen vector and 'l_i' is the 'i^{th}' row left Eigen vector. Eigen value 'λ_i' and corresponding 'r_i' and 'l_i' define the 'i^{th}' mode of Q-V response. The relationship between left and right Eigen vectors can be written as Equation (2.20).

$$\underline{R}^{-1} = \underline{L} \tag{2.20}$$

Substituting Equation (2.20) in Equation (2.10), we obtain Equation (2.21).

$$\underline{L}\,\underline{\Delta V} = \underline{\Lambda}^{-1}\underline{L}\underline{\Delta Q} \tag{2.21}$$

$$\underline{v} = \underline{\Lambda}^{-1}\underline{q} \tag{2.22}$$

Where $\underline{v} = \underline{L\Delta V}$ is vector of modal voltage analysis and $\underline{q} = \underline{L}\underline{\Delta Q}$ is vector of modal reactive power variations.

From Equation (2.22), we can write Equation (2.23).

$$v_i = \frac{1}{\lambda_i} q_i \tag{2.23}$$

And $\underline{\Lambda}^{-1}$ is diagonal matrix. Details of development of Equation (2.13) to (2.22) is provided in [**1**].

From above equations it is clear that if $\lambda_i > 0$ then the voltage and reactive power of the i^{th} mode are along the same direction which implies that voltage stable. If $\lambda_i < 0$, the voltage and reactive power of i^{th} mode are along opposite direction which implies voltage unstable. The magnitude of λ_i determines the degree of stability of the i^{th} modal voltage. A smaller magnitude of positive λ_i means that the i^{th} mode is closer to voltage instability and vice versa. If $\lambda_i=0$ it means that i^{th} modal voltage collapses.

2.2 Dynamic Analysis

The dynamic analysis of voltage stability will be the same as transient stability because the structures for dynamic analysis are the same as transient stability structure. The whole system representation can be done with a set of first order differential and algebraic equations. These equations can be solved in time-domain by using numerical integration techniques. The study has to be typically done in orders of several minutes. The order of the differential equation can be reduced by introducing time-scale decomposition techniques. The methods to divide dynamics or reducing the order of the differential equations on the basis of the operating time-span of the power system equipment will be discussed later in this section.

Power system has equipment which operates in different time spans in response to a disturbance in the system. All of these devices will contribute towards system dynamics. Because of this equipment, voltage instability and collapse dynamics will span a range in time from a fraction of second to tens of minutes.

Figure 2.3 show that many power system components and controls play an important role in voltage stability. All the equipment shown in Figure 2.3 will not contribute to a particular voltage collapse incident or scenario, the system characteristics and the disturbance will determine that important phenomenon.

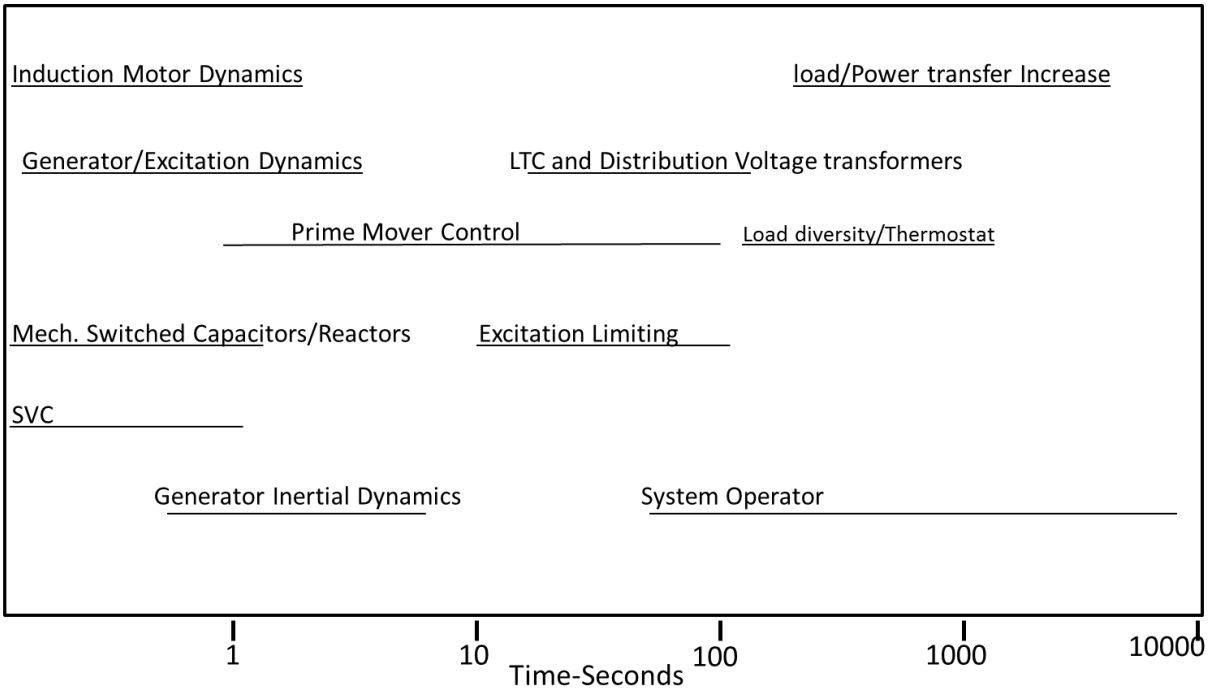

Figure 2.3: Operational time frame of equipment in power systems [**2**]

Power system dynamics can be divided into three time-scale dynamic types based on the operating time of the equipment. Those are [**14**]:

1. Instantaneous response
2. Short-term dynamics
3. Long-term dynamics

A simple four bus system, shown in Figure 2.4, is used as an example to describe all the above mentioned dynamics. This simple power system includes a synchronous generator, motor tap changing transformer and capacitor bank to cover all the dynamic response ranges.

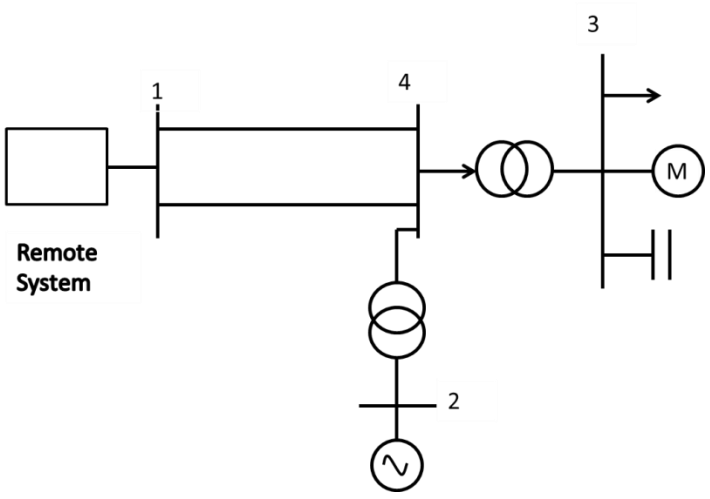

Figure 2.4: One line diagram of a simple four bus power system [**14**]

Figure 2.5 is the circuit representation of the four bus system shown in Figure 2.4 with all the transmission lines and transformers represented by a pi-equivalent model.

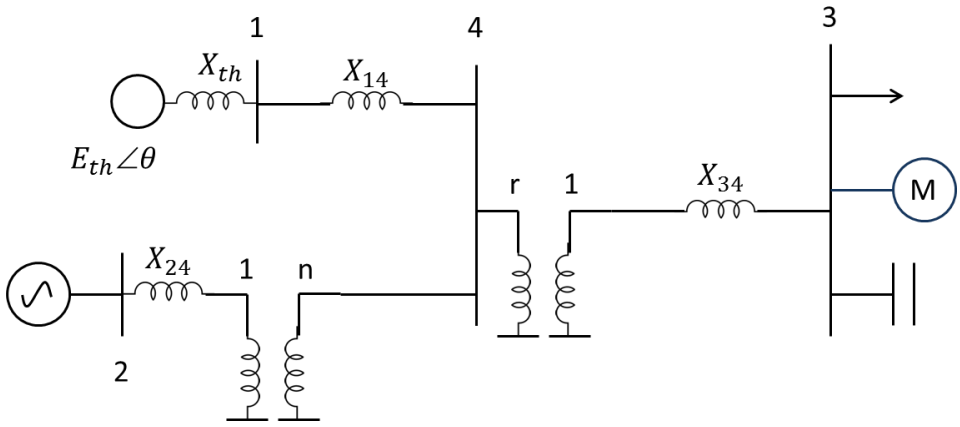

Figure 2.5: Circuit equivalent representation of four bus power system

Network equations are assumed to be instantaneous for voltage stability studies. Since the electromagnetic transients are very fast relative to the interested time span for voltage stability

studies. The instantaneous response for network equations which are differential in nature can be reduced to become algebraic equations with this assumption. These equations can be represented mathematically as Equation (2.24).

$$0 = \underline{g}(\underline{x}, \underline{y}, \underline{z}_c, \underline{z}_d) \tag{2.24}$$

Where $\underline{y}$ is vector of bus voltages. Variables $\underline{x}$, $\underline{z}_c$, $\underline{z}_d$ will be defined later in this section.

The network equations assumed as instantaneous response for the system shown in Figure 2.5 are given in Equations (2.25) to (2.28).

$$\frac{E_{th}\angle\theta_{th} - V_1}{X_{th}} - Y_{14}(V_1 - V_4) = 0 \tag{2.25}$$

$$I_2 - Y_{24}(V_2 - V_4) - Y_{s24}V_2 = 0 \tag{2.26}$$

$$I_3 - Y_{34}(V_3 - V_4) - Y_{s34}V_3 = 0 \tag{2.27}$$

$$Y_{14}(V_4 - V_1) + Y_{24}(V_2 - V_4) + Y_{34}(V_3 - V_4) - V_4(Y_{s42} + Y_{s43}) = 0 \tag{2.28}$$

Where $V = |V|\angle\theta$, $Y = G + iB$, and $I = |I|\angle\emptyset$. Variables for the instantaneous response represented by vector $\underline{y}$ are V_1, V_2, V_3, and V_4. Y_{ij} represent the admittance of the line connecting Node *i* to Node *j*. It is not the element of the Y_{BUS} matrix. All parameters and variables are complex numbers represented in their polar form.

Short-term dynamic responses contributed by the equipment operating in seconds after the disturbance are shown in Figure 2.3. They include synchronous generators and their automatic voltage regulators(AVR) and governors, induction motors, HVDC components and

SVCs. These short term dynamic responses will last typically for several seconds following the disturbance. The short dynamics are captured mathematically by differential Equation (2.29).

$$\dot{\underline{x}} = \underline{f}(\underline{x}, \underline{y}, \underline{z}_c, \underline{z}_d) \tag{2.29}$$

The short-term dynamic equations for synchronous generators, AVRs, and induction motors contributing to Equation (2.29) for the system shown in Figure 2.4 and Figure 2.5 are given in Equation (2.30) to (2.34).

- Generator dynamics

$$\dot{\delta} = \omega \tag{2.30}$$

$$\dot{\omega} = -\frac{D}{2H}\omega + \frac{\omega_0}{2H}(P_m - P_2) \tag{2.31}$$

$$\dot{E}_q{}' = \frac{-E_q{}' + v_{fd} - (X_d - X_d{}')i_d}{T_{do}{}'} \tag{2.32}$$

- AVR dynamics

$$\dot{v}_{fd} = 0 \; if v_{fd} = v_{fd}^{max} \; and \; G(V_{2o} - V_2 - x_{oxl}) - v_{fd} > 0 \tag{2.33}$$

$$= 0 \; if v_{fd} = v_{fd}^{min} \; and \; G(V_{2o} - V_2 - x_{oxl}) - v_{fd} < 0$$

$$= \frac{-v_{fd} + G(V_{2o} - V_2 - x_{oxl})}{T} \; otherwise$$

- Induction motor dynamics

$$\dot{s} = \frac{1}{2H}(T_M - P_M) \tag{2.34}$$

The state variables (x) for short-term dynamics shown in Equation (2.30) to (2.34) are δ, ω, $E_q{}'$, v_{fd}, and s.

The time frame for long-term dynamics is typically measured in minutes and corresponds to the time scale of the phenomenon, controllers, and protecting devices that typically act over several minutes following a disturbance. The controllers and protecting devices are generally designed to act after the short-term dynamics have died out to avoid unnecessary or even unstable interactions with short-term dynamics. The device contributing towards long-term dynamics are,

- Phenomenon- Thermostatic load recovery and aggregate load recovery.
- Controllers- Secondary voltage control, load-frequency control, load tap changers (LTCs) and shunt capacitor/reactor switching.
- Protecting Devices- over excitation limiters (OXLs) and armature current limiters.

The long-term dynamics are represented by both continuous and discrete-time Equations (2.35) and (2.36) respectively.

$$\dot{\underline{z}}_c = \underline{h}_c(\underline{x}, \underline{y}, \underline{z}_c, \underline{z}_d) \tag{2.35}$$

$$\underline{z}_d(k+1) = \underline{h}_d(\underline{x}, \underline{y}, \underline{z}_c, \underline{z}_d(k)) \tag{2.36}$$

The long-term dynamic equations for over excitation limiters and load tap changing transformers contributing to Equation (2.35) and Equation (2.36) for the system shown in Figure 2.4 and Figure 2.5 are given as Equations (2.37) and (2.38).

- Over-Excitation limiter dynamics- Long-term continuous

$$\dot{x}_t = 0 \text{ if } x_t = K_2 \text{ and } x_2 \geq 0 \qquad (2.37)$$

$$= 0 \text{ if } x_t = -K_1 \text{and } x_2 < 0$$

$$= x_2 \text{ otherwise}$$

- Load tap changer dynamics- Long-term discrete

$$r_{k+1} = r_k + \Delta r \; if V_3 > V_{3o} + d \; and \; r_k < r^{max} \qquad (2.38)$$

$$= r_k - \Delta r \; if V_3 < V_{3o} - d \; and \; r_k < r^{min}$$

$$= r_k \; otherwise$$

Variables for long term continuous dynamics are x_t and Variables for long term discrete dynamics are r.

2.2.1 Time-Scale Decomposition

The previous section described three types of time-scale dynamics in a modern power system. The following section will provide a perspective on how to deal with these multiple time-scale dynamics in power systems.

One can deal with multiple time-scale dynamics with whole sets of differential-algebraic, discrete-continuous time equations in digital simulations by using modern computer technology. But to better understand voltage instability mechanisms, and to improve efficiency by utilizing faster analysis methods, it is advantageous to exploit the time separation between short and long

term dynamics. By using time-scale separation, fast component models can be derived by considering that slow states are practically constant during fast transients. In the same manner, slow component models can be derived by assuming fast transients do not exist during slow changes. With the availability of multi-time-scale models, one can derive accurate, reduced-order models suitable for each time scale. This process is called time-scale decomposition [**14**]. Time-scale decomposition is based on the analysis known as singular perturbation.

For a singular perturbed system, a small parameter ε multiplies one or more state variables. Substituting ε=0 will change the order of the system. Mathematically, a singular perturbed system can be shown as Equations (2.39) and (2.40).

$$\underline{\dot{x}} = \underline{f}(\underline{x}, \underline{y}, \varepsilon) \tag{2.39}$$

$$\varepsilon\underline{\dot{y}} = g(\underline{x}, \underline{y}, \varepsilon) \tag{2.40}$$

By applying time-scale decomposition on Equations (2.39) and (2.40), one can derive two reduced order systems, such that one describes slow dynamics and other fast dynamics.

$$\underline{x} = \underline{x}_s + \underline{x}_f \tag{2.41}$$

$$\underline{y} = \underline{y}_s + \underline{y}_f \tag{2.42}$$

Here $\underline{x}_s$, $\underline{y}_s$ and x_f, $\underline{y}_f$ are slow and fast components of the state variables.

The small parameter ε in front of Equation (2.40) shows that the dynamics of $\underline{y}$ are faster than those of $\underline{x}$. Deriving approximations of the slow dynamics is done by setting ε=0. This

defines a quasi-steady state (QSS) approximation of the slow sub system as shown in Equations (2.43) and (2.44).

$$\dot{\underline{x}} = \underline{f}(\underline{x}_s, \underline{y}_s) \tag{2.43}$$

$$0 = \underline{g}(\underline{x}_s, \underline{y}_s) \tag{2.44}$$

Figure 2.6 illustrates the concept of applying time-scale decomposition to power system Equations (2.24), (2.29), (2.35), and (2.36).

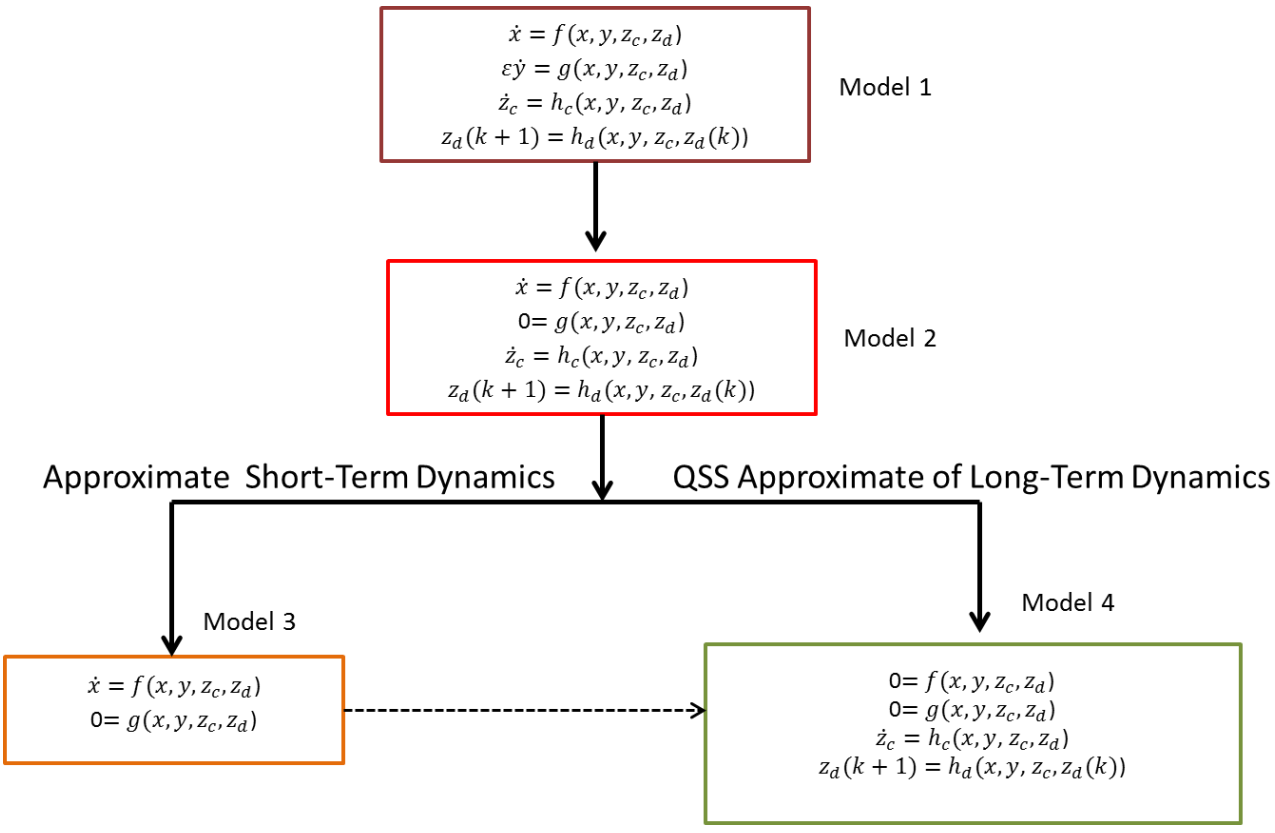

Figure 2.6: Time-scale decomposition [**14**]

Figure 2.6 shows that by assuming an instantaneous response for the network, the power system equations in model 1 will reduce to the equations in model 2. By applying the time-scale decomposition technique, short dynamics can be further approximated to model 3 based on the assumption that slow components are not reacting for short dynamics or fast dynamics. Likewise QSS approximations for long term dynamics can be obtained using model 4 since fast dynamics become vanished when long term dynamics are acting.

This time-scale decomposition section is provided to allow the reader to better understand the importance of modeling and to provide an idea of how system solutions can be achieved by using more efficient methods resulting in tremendous time saving. This time saving, however, comes at the cost because it may lead to the less accurate dynamic system models and will result in erroneous result. Utilizing the proposed methodology in this dissertation will achieve faster and better resolution in finding system voltage abnormalities. This is because the main purpose of this research is to analyze dynamic behavior of a stressed power system based on performing the dynamic computer simulations or receiving real-time data from PMUs and then correlating the dynamic responses to determine the future system voltage abnormality.

The reminder of the dissertation includes stating the objectives and outline of the methodology in Chapter 3, modeling of test system in Chapter 4, providing the results and voltage stability prediction analysis for the test system in Chapter 5, and in Chapter 6, concluding with the summary of this dissertation and discussion of future work.

This dissertation will now proceed to the objective and methodology of the proposed technique to detect voltage abnormality in Chapter 3.

Chapter 3

3 Problem Statement, Objective, and Methodology

The previous chapters have given an insight into power system stability, voltage instability, voltage collapse, and the existing methods used to detect voltage collapse in power systems. This chapter will summarize the difficulties in detecting voltage collapse, and the approach taken by this research to analyze the dynamic behavior of a stressed power system and to correlate the dynamic responses to a future system voltage abnormality.

The purpose of this dissertation is to analyze dynamic behavior of a stressed power system and to correlate the dynamic responses to the future system voltage abnormality. It is postulated that the dynamic response of a stressed power system in a short period of time - in seconds - contains sufficient information that will allow prediction of voltage abnormality in future time - in minutes [**40**] [**42**]. The software package PSSE Dynamics simulator is used to study the dynamics of the IEEE 39 Bus equivalent test system. To correlate dynamic behavior to system voltage abnormality, this research utilizes an algorithmic pattern recognition method called Regularized Least Square Classification (RLSC) and a statistical method called Classification and Regression Tree (CART).

3.1 Problem Statement: Complications in Detecting Voltage Collapse

Voltage collapse may occur in several different ways. In complex practical power systems, many factors contribute to the process of system collapse because of voltage instability: strength of transmission system, power transfer levels, load characteristics, generator reactive power capabilities, and characteristics of reactive compensating devices. In some cases, the problem is

compounded by uncoordinated action of various controls and protective devices. It is very difficult to detect voltage collapse ahead of time. Listed below are some of the general characteristics which make it complicated to detect voltage collapse:

- Voltage collapse is a dynamic phenomenon. Section 2.2 has given an insight into the power system dynamics and their effect on voltage collapse.
- Voltage collapse can be initiated by variety of causes from large sudden disturbances like loss of generating units or loss of heavily loaded lines, to small system variations like natural increase in system load.
- Voltage collapse is a cascading phenomenon. An initial disturbance may lead to successive tripping of multiple resources in the power system and eventually will lead to voltage collapse.
- The process of voltage collapse involves many automatic and manual controls like system protection relays, load tap changers, generator prime mover controls and voltage regulators, as well as series and shunt capacitors.
- Voltage collapse is a slow and fast phenomenon. Time taken for the voltage collapse varies with case by case and system to system after the initial disturbance. Section 1.5 covers a few major blackouts occurring in the past. These events have shown that time taken for voltage collapse varies case by case.

All of the above mentioned characteristics leading to voltage collapse complicate the process of detecting voltage collapse ahead of time. If the voltage collapse is detected at earlier stages one can take remedial actions to prevent power system from voltage collapse.

3.2 Objective

The main objective of this research is to predict the voltage collapse ahead of time to provide the operators a lead time for remedial actions and for possible prevention of blackouts. This research analyzes dynamic behavior of a stressed power system and correlates the dynamic responses to the future system voltage abnormality. It is postulated that the dynamic response of a stressed power system in a short period of time - in seconds - contains sufficient information that will allow prediction of voltage abnormality in future time - in minutes.

3.3 Methodology

As discussed in the previous sections, the main objective of this research is to detect voltage collapse ahead of time. The methodology to achieve this objective consists of three phases which are shown in the flow chart of Figure 3.1.

1. Modeling and simulation of test system: capture the power system dynamic response.
2. Data Processing and feature extraction: extract the system variables around the instance of a disturbance that includes some pre-disturbance and post-disturbance variables.
3. Classification of voltage abnormality: apply pattern recognition techniques.

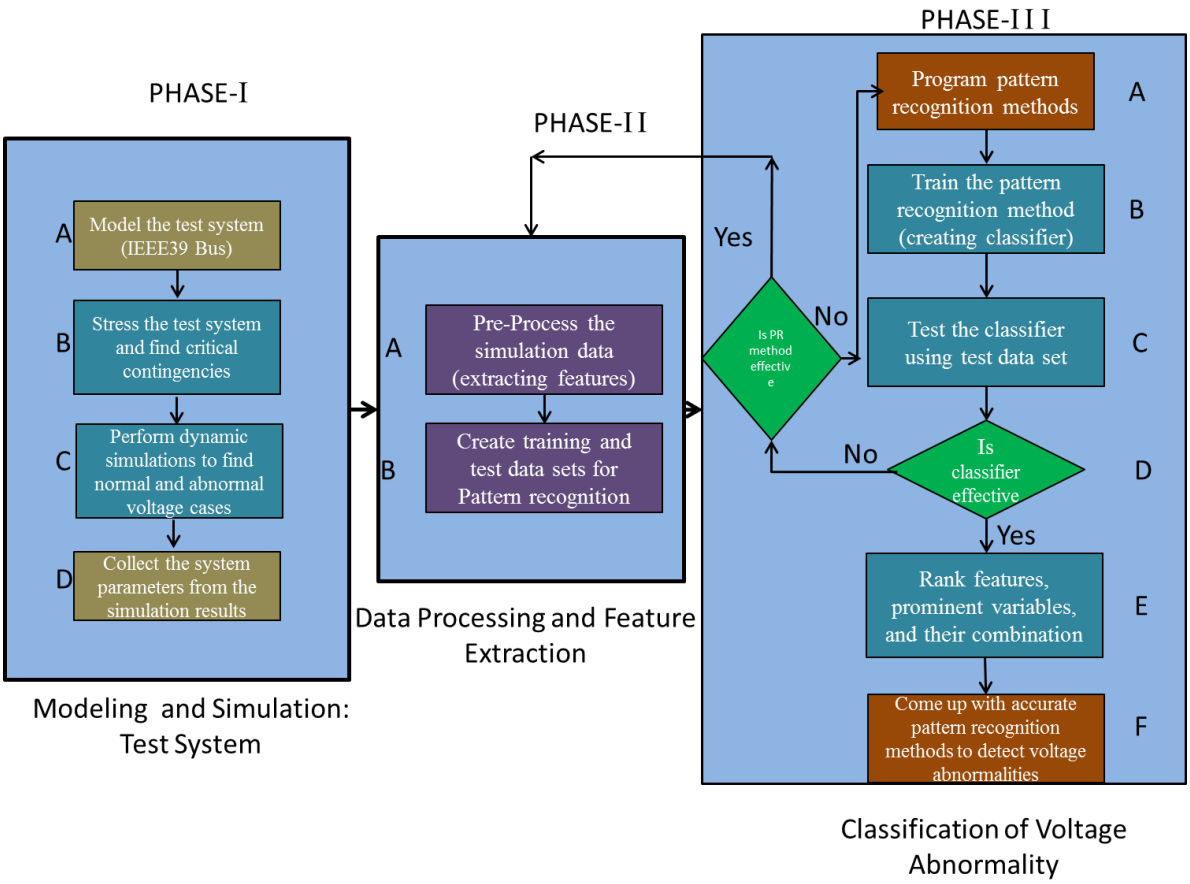

Figure 3.1: Methodology flowchart for voltage stability prediction

3.3.1 Modeling and Dynamic Simulation of Test System (Phase-I)

Phase-I of the methodology discussed earlier in Section 3.2 is to capture the dynamic response of the system. Here capturing the system response means recording the system variables like bus voltage magnitudes, voltage angles, real and reactive powers, and generator rotor angles. Dynamic response of the system can be captured by any one of the following two methods,

1. Using the equivalent system models and dynamic simulation tools

- Model the equivalent system for dynamic simulations in power system simulation tools such as PSSE.
- Perform the dynamic simulations on the modeled system using dynamic simulation tools.
- Capture the system response for all the variables of the system

2. Collecting data from the field using PMUs
    - Capture system data from the phasor measurement units (PMU) installed in the substations. These PMUs will record system variables with time stamp synchronized to GPS time clock.

To test the proposed methodology, this research utilized the IEEE 39 Bus equivalent system in detecting voltage instability. This research can only use the first method from the above mentioned two methods to capture the dynamic response on the test system. Flow chart shown in Figure 3.1 shows all the steps involved in Phase-I.

Phase-I has four steps to capture the test system dynamic response. Test system is modeled in Phase-I: Step A. Flow chart for this step is shown in Figure 3.2. In this step the equivalent model data for the test system is collected from different articles and books, and is modeled in power system dynamic simulation software such as PSSE. Multiple equivalent system models are created with different types of loads like induction motor loads, composite load models, and ZIP load models. Once the system models are built, a dynamic simulation is performed on the system model for a base case (without applying any contingency). If the system dynamic response is stable then the tasks in the next step of Phase-I will be performed.

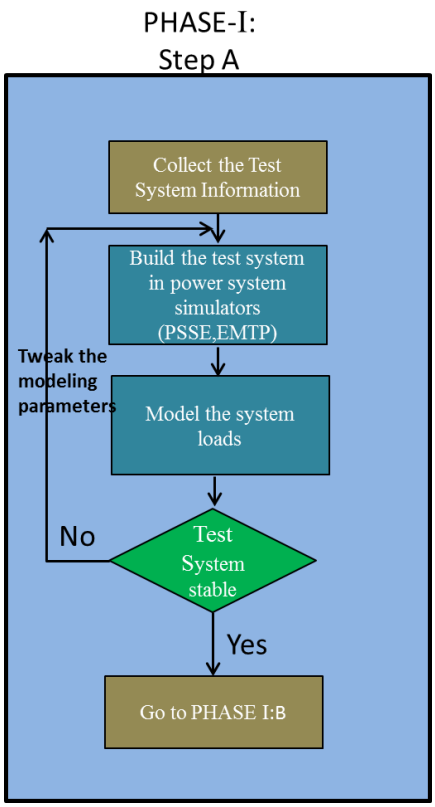

Figure 3.2: Flow chart for Phase-I: Step-A

In Phase-I: Step-B, test system is stressed to determine critical contingencies by increasing load or disconnecting generating plants or disconnecting transmission lines. Flow chart for Phase-I: Step-B is shown in Figure 3.3. Contingency analysis is performed to determine the critical contingencies, and from those contingencies voltage stable and voltage unstable cases will be determined.

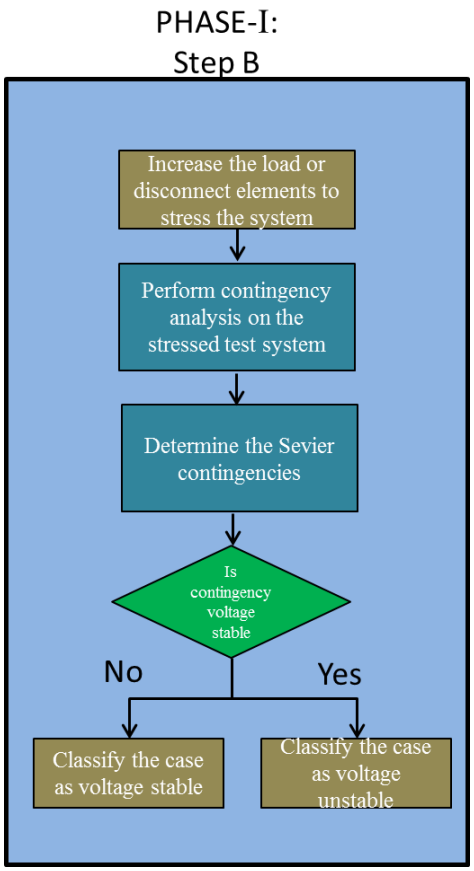

Figure 3.3: Flow chart for Phase-I: Step-B

After determining the critical contingencies, dynamic simulations are performed on voltage stable and voltage unstable cases in Phase-I: Step-C using the power system dynamic simulation software. Flow chart for Phase-I: Step-C is shown in Figure 3.4. Initially the base case will be prepared for dynamic simulations, then dynamic simulations are performed on the contingencies found in Phase-I: Step-B and system parameters are captured. Voltage stability is determined from the dynamic simulations performed on each contingency. In Phase-I: Step-D system parameters or variables such as bus voltage magnitudes, voltage angles, real and reactive powers, and generator rotor angles are collected.

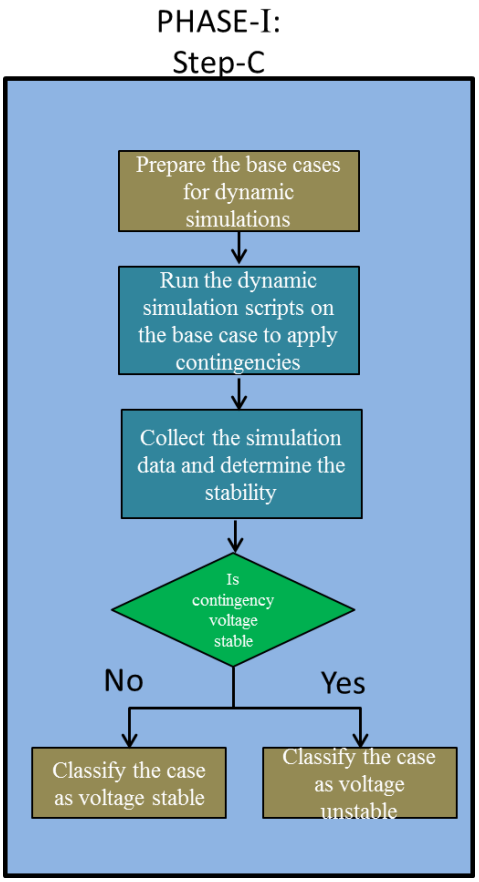

Figure 3.4: Flow chart for Phase-I: Step-C

3.3.2 Data Processing and Feature Extraction (Phase-II)

Phase-II of the proposed methodology has two stages to pre-process the captured system dynamic response for Phase-III. Flow chart shown in Figure 3.1 shows the stages for Phase-II. Simulation parameters are extracted from the captured dynamic response of the system around the disturbance. This extracted system variables have a few seconds of the system dynamic response for pre-disturbance and post-disturbance data. Flow chart shown in Figure 3.5 shows the process for Phase-II: Step-A. Multiple features are prepared from the extracted data. These features are divided into training and test samples for Phase-III.

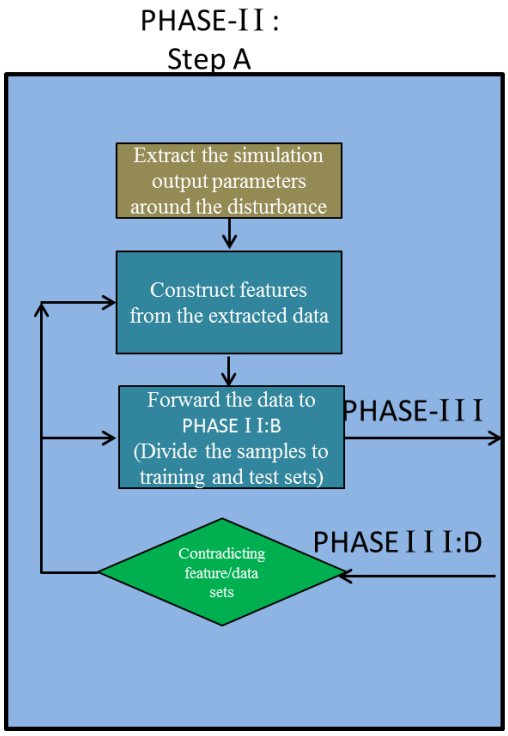

Figure 3.5: Flow chart for Phase-II: Step-A

3.3.3 Classification of Voltage Abnormality (Phase-III)

The last phase of the proposed methodology uses the pattern recognition techniques to predict the voltage stability from the power system dynamic response. Flowchart for Phase-III is shown in Figure 3.1. Algorithmic and statistical pattern recognition techniques are programmed in this phase. These programmed methods are trained using the training samples extracted from Phase-II and a classifier to predict voltage stability is developed from the pattern recognition methods. This classifier is tested with the test samples extracted from Phase-II. If prediction using the classifier is accurate and efficient, then the prominent features and prominent system variables leading to this stability prediction are determined. If the developed classifier from pattern recognition method is not accurate, then problems relating to this defective classifier,

either the pattern recognition method or the training samples used to train the pattern recognition method, are determined and corrected. In the last stage of Phase-III the accurate pattern recognition methods to predict voltage collapse are determined.

3.4 Pattern Recognition

According to Duda and Hart [**43**], "pattern recognition is act of taking in raw data and taking an action based on the category of the pattern". A pattern is a type of reoccurring event or object which can be named. Finger print image, hand written word, and speech are examples of a pattern. The process of recognition is a machine classification and assigns the given objects to prescribed classes. Figure 3.6 illustrates the flow chart pattern recognition model development and data classification.

Pattern recognition techniques are used in engineering applications like wave form classification where wave forms corresponding to one class of data are discriminated from the data corresponding to a different class. We are using pattern recognition techniques to distinguish voltage stable waveforms from voltage unstable waveforms. Regularized least-squares (RLS) classification is used for our binary classification problem. RLSC is a learning method that obtains solutions for binary classification problems.

By looking at Figure 3.6 it can be observed that pre-processing will take place on the training set and test set acquired data and is forwarded to feature extraction purpose. Features will be chosen on the given data. These selected features from the training set data are used to build an optimized model for estimation. Later this model will be used to classify the patterns of the test set data.

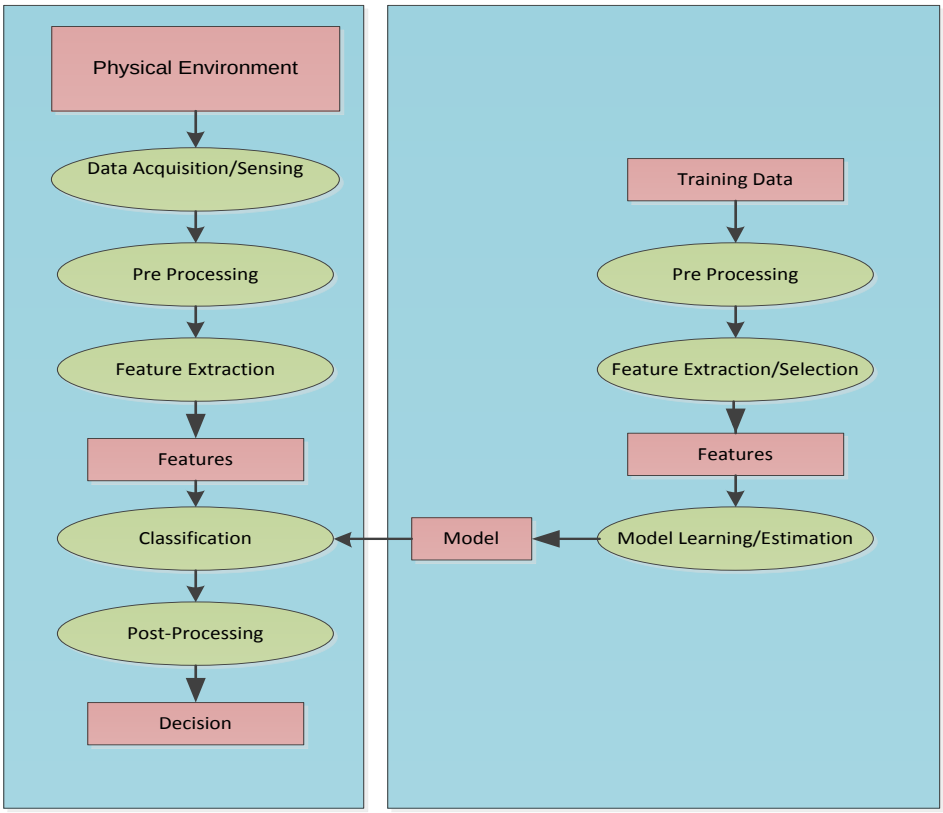

Figure 3.6: Flow Chart of Pattern Recognition Model [**40**]

3.4.1 Regularized Least-Square Classification (RLSC)

As mentioned earlier RLSC is a learning method that obtains solutions for binary classification via Tikhonov regularization in a Reproducing Kernel Hilbert Space using the square loss function [**44**] [**45**]. Let's assume X and Y are two sets of random variables and training set for pattern classification is S = (x_1, y_1), …., (x_n, y_n) and it satisfies $x_i \epsilon R^n$ and $y_i \epsilon \{-1, 1\}$ for all i. the main goal is to learn a function *f(x)* while minimizing the probability of error described by Equation 2.42.

$$\Pr\left(sgn\left(f(x)\right)\right) \neq y \qquad (3.1)$$

To minimize the error we can use Empirical Risk Minimization (ERM) and obtain M_1 such that

$$M_1 = \min_{f \epsilon H} \frac{1}{n} \sum_1^n \big(y_i - f(x_i)\big) \qquad (3.2)$$

Above problem is ill defined, because the set of functions required in minimizing Equation 3.2 is not considered. By representing function *f* that lies in a bounded convex subset of a Reproducing Kernal Hibert Space H that simultaneously has small empirical error and small norm in reproducing Kernel Space generated by kernel function K. The resulting minimization problem can be solved via Lagrange multipliers.

$$\mathrm{M}_2 = \min_{f \epsilon H} \frac{1}{n} \sum_1^n \big(y_i - f(x_i)\big)^2 + \lambda \|f\|^2{}_k \qquad (3.3)$$

where $\|f\|^2{}_k$ is the norm in the hypothesis space defined by kernel k.

Solution to Equation 3.3 is indexed by the tuning parameter λ. The tuning parameter controls the amount of regularization so it is crucial to choose a good tuning parameter. This research uses Tibshirani's Least Absolute Shrinkage and Selection Operator (LASSO) [**46**]. LASSO coefficients are the solutions to the ℓ1 optimization problem. LASSO will seek for a sparse solution such that choosing the large enough λ which will set some coefficients to zero.

The solution for Tikhonov regularization problem can be solved by Representer Theorem [**47**] [**48**] and it is:

$$f(x) = \sum_{i=1}^n c_i k(x, x_i) \qquad (3.4)$$

Learning algorithm for this problem is very simple. First kernel matrix K is constructed from training set S.

$$K = \left(k_{ij}\right)_{1 \le i,j \le n} \qquad k_{ij} = k\left(x_i, x_j\right)$$

Next step is to compute the vector coefficients c= $(c_1, c_2, \ldots, c_n)^T$ by solving the system of linear equations

$$(K + n\lambda I)c = y \tag{3.5}$$

$$c = (K + n\lambda I)^{-1} y \tag{3.6}$$

Where y = $(y_1, \ldots, y_n)^T$ and I is the identity matrix of dimension n, and finally classifier is,

$$f(x) = \sum_{i=1}^{n} c_i k(x, x_i) \tag{3.7}$$

The sgn (f(x)) will give the predicted label (-1 or +1) for the instance x whereas magnitude of f(x) is the confidence in this prediction.

3.4.2 Classification and Regression Trees (CART) - Data Mining

Data mining is the process of extracting knowledge from data. The goal is to extract rules or knowledge from regularity patterns exhibited by the data. Decision Trees (DTs) is a method used for Data Mining. This research uses CART (Classification and Decision Trees) methodology to build the DTs. Here Salford System's data mining software CART® is used in the voltage stability analysis.

A Decision Tree is a form of inductive learning. For a given data set, the objective is to build a model that captures the mechanism that gave rise to the data. The process of constructing the model is a "Supervised learning" problem since the training is supervised by an outcome

variable called the target [**49**]. Figure 3.7 shows a schematic view of a decision tree. Decision Trees are grown through a systematic method known as recursive binary partitioning; where successive questions with yes/no answers are asked in order to partition the sample space.

The process begins with a "root" node that encloses the learning sample *L*. At each node *t* the sample is split into two subsets t_L and t_R, the left and right child respectively. The splitting process is iterated until the terminal node is reached, i.e. a node where no further split is possible. A classification decision is made at such terminal nodes.

The learning sample L is composed by a set of measurements vectors $X = \{x_1, x_2, \dots, x_m\}$. Each column of a measurement vector x_i is known as an attribute. An attribute can be either numerical or categorical. Categorical attributes take a finite set of values and do not have an intrinsic order; for example: temperature = {cold, hot}. On the other hand, numerical attributes take value in a real line and therefore have a natural order.

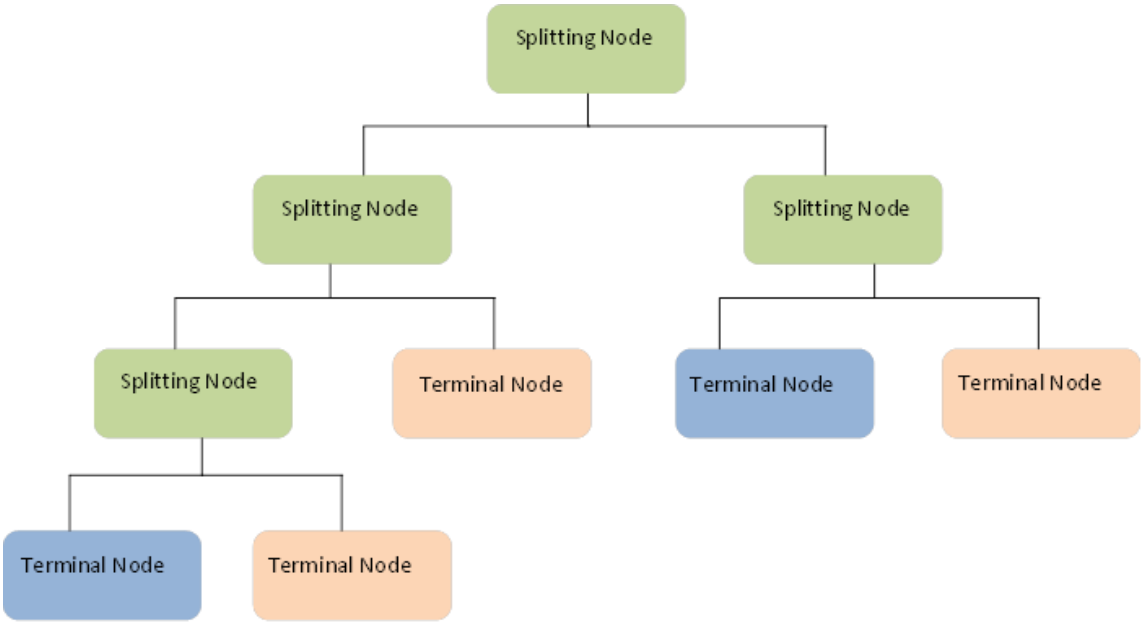

Figure 3.7: Classification Trees - After a successive sample partitions, a classification decision is made at the terminal nodes

Being a supervised learning method, the class of each vector must be known prior to data mining process. Therefore, each measurement vector x_i must be classified into a set of mutually exclusive classes $C = \{C_1, C_2, \ldots, C_J\}$.

Table 3.1 Learning sample matrix with n attributes and m measurement vectors

	Target	Attr 1	Attr 2	Attr 3	. . .	Attr n
$\boldsymbol{x_1}$	C_j	numerical	categorical	. . .	. . .	. . .
$\boldsymbol{x_2}$	. . .	. . .	. . .	. . .	. . .	. . .
.	.	.	.	.	.	.
.	.	.	.	.	.	.
.	.	.	.	.	.	.
$\boldsymbol{x_m}$	. . .	. . .	. . .	. . .	. . .	. . .

In general, the learning sample L is a matrix with m rows (the number of measurement vectors) and $n + 1$ columns (the number of attributes on each measurement vector plus the target).

As mentioned earlier the process begins at the root node which encloses the learning sample L. The idea is to partition the space into disjoint subsets so as to increase the "purity". Purity can be understood as a measurement of class homogeneity. Homogeneous nodes that include only one class C_j achieve maximum purity, whereas heterogeneous nodes with an equal proportion of classes $C_0, \dots, C_j$ have minimum purity.

A split is said to be optimal when it maximizes the purity of the descendent nodes. For convenience, optimality can be expressed in terms of node impurity rather than purity. In this case, optimal split should minimize the impurity. Gini index, Entropy Impurity, Towing are some of the impurity functions generally used [**49**]. The most commonly used index is called "Gini Impurity index", and is defined as follows:

$$i(t) = 1 - \sum_{j}^{J} p^2(C_j|t) \tag{3.8}$$

where $p(C_j|t)$ is an estimator of the probability that a case belongs to class C_j given that it falls into t.

Then, the goodness-of-split criterion of a split s at node t is defined to be the decrease in impurity achieved by split s,

$$\Delta i(s,t) = i(t) - [\, p_L . i(t_L) + p_R . i(t_R)] \qquad (3.9)$$

where $i(t)$ is impurity measurement at node t computed using equation (3.8), p_L and p_R are the proportion of cases that fall into the left and right child respectively, and $i(t_L)$ and $i(t_R)$ are the left and right child impurity measurements.

The optimal split $\boldsymbol{s_{optimal}}$ is defined to be the split that maximizes the decrease in impurity in equation (3.9). To find such a split, CART performs an exhaustive search over all attributes and all possible splitting values.

Let us consider the set of attributes $A = \{a_1, a_2, \dots, a_n\}$. Each attribute $a \in A$ is iteratively selected one at a time. If the selected attribute is numerical, then there is an infinite number of possible splitting values. It is customary, though completely arbitrary, to select the midpoint between two adjacent values splitting rule. If the selected attribute is categorical, then there is a finite number of splitting thresholds and they are set of unique categories in A.

Let us define $S_a = \{s_1, s_2, \dots\}$ to be the set of potential splitting values of attribute a. The optimal split s_a of attribute a is the one that maximizes the decrease in impurity expressed by equation (3.9). Finally, $\boldsymbol{s_{optimal}}$ at node t is the split that maximizes the decrease in impurity $\Delta i(s,t)$ over all the attributes $a \in A$ and splitting values $s \in S_a$.

Following this systematic procedure, the tree is grown by recursively finding optimal splits and partitioning each node into two children. CART's algorithm initially grows a tree as large as possible. A node is considered to be terminal if it has achieved zero impurity or if the total number of measurement vectors x_i at node t is less than some predetermined value n_{min}.

Finally, a classification decision is made at the terminal nodes. Class C_j is assigned to terminal node if $p(C_j|t)$ is the largest,

$$p(C_j|t) = \max_i(p(C_i|t)) \tag{3.10}$$

Voltage normal and voltage abnormal cases are simulated using PSSE dynamics tool and the results of simulation from PSSE dynamics will be divided into two sets of training and testing set data. Each of the two sets of data includes both voltage normal and voltage abnormal cases that are used for development and validation of a discriminator. Then the stressed system simulation results are used to train two pattern recognition models RLSC and CART using the training set obtained from the dynamic simulation data. After the training phase, the trained pattern recognition algorithm will be validated using the remainder of data obtained from simulation of the stressed system. This process will determine the prominent features and parameters in the process of classification of voltage normal and voltage abnormal cases from dynamic simulation data. These results will be provided in the Chapter 5 of this document.

The remainder of the dissertation includes traditional methods for determining modeling of test system in Chapter 4, results and voltage stability prediction analysis on test system in Chapter 5, and the summary of this dissertation and future work presented in Chapter 6.We now proceed to the test system modeling and dynamic simulation in Chapter 2.

Chapter 4

4 Test System

4.1 IEEE 39 Bus Test system

The IEEE 39 BUS (NEW ENGLAND) equivalent power system is used to study the voltage stability dynamics. This test system has a total of 39 buses of which 10 buses are generator buses. This system has a total of 19 loads at different buses and includes 12 transformers, 10 generators and 34 transmission lines. This system is shown in figure (4.1). This chapter will provide the information about the test system in a form of that PSSE can accept the data.

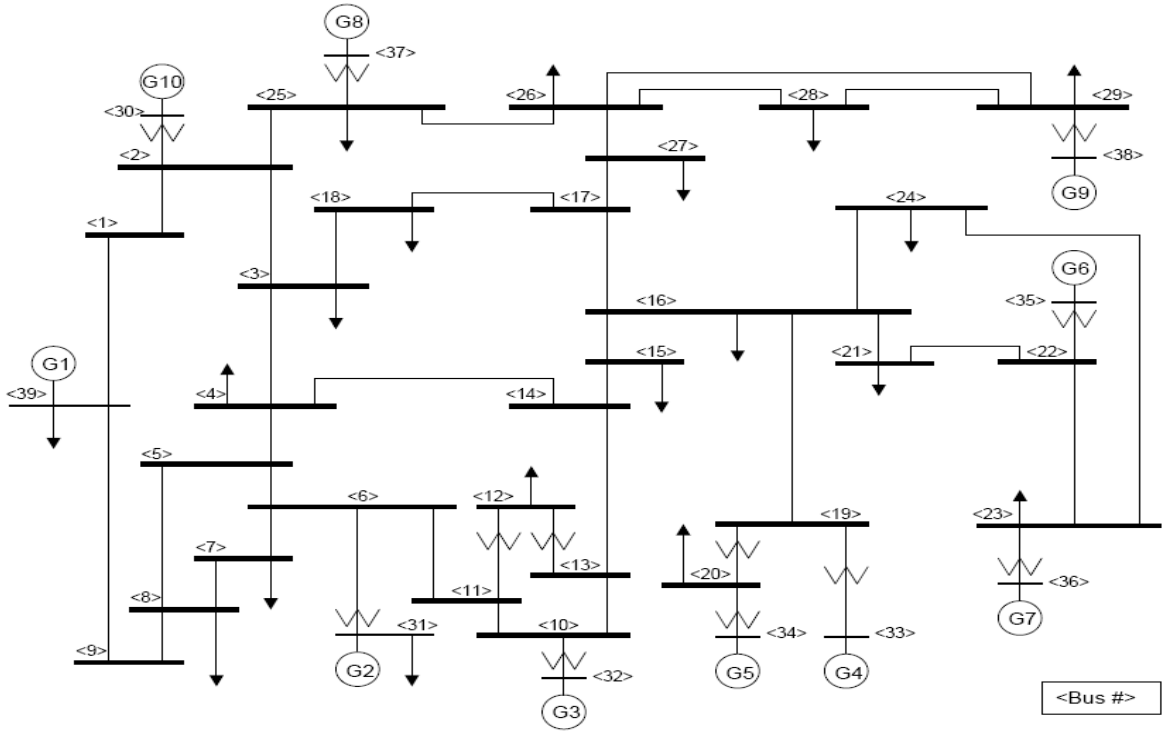

Figure 4.1 IEEE 39 Bus System [**50**]

4.2 Transmission Lines

Table 4.1 Transmission Line Data

Line	Resistance PU	Reactance PU	Suceptance PU
1 to 2	0.0035	0.0411	0.6987
1 to 39	0.001	0.025	0.75
2 to 3	0.0013	0.0151	0.2572
2 to 25	0.007	0.0086	0.146
3 to 4	0.0013	0.0213	0.2214
3 to 18	0.0011	0.0133	0.2138
4 to 5	0.0008	0.0128	0.1342
4 to14	0.0008	0.0129	0.1382
5 to 6	0.0002	0.0026	0.0434
5 to8	0.0008	0.0112	0.1476
6 to 7	0.0006	0.0092	0.113
6 to 11	0.0007	0.0082	0.1389
7 to 8	0.0004	0.0046	0.078
8 to 9	0.0023	0.0363	0.3804
9 to 39	0.001	0.025	1.2
10 to 11	0.0004	0.0043	0.0729
10 to 13	0.0004	0.0043	0.0729
13 to 14	0.0009	0.0101	0.1723
14 to 15	0.0018	0.0217	0.366
15 to 16	0.0009	0.0094	0.171

Continued…

Table 4.1 Continued

16 to 17	0.0007	0.0089	0.1342
16 to19	0.0016	0.0195	0.304
16 to 21	0.0008	0.0135	0.2548
16 to 24	0.0003	0.0059	0.068
17 to 18	0.0007	0.0082	0.1319
17 to 27	0.0013	0.0173	0.3216
21 to 22	0.0008	0.014	0.2565
22 to 23	0.0006	0.0096	0.1846
23 to 24	0.0022	0.035	0.361
25 to 26	0.0032	0.0323	0.513
26 to 27	0.0014	0.0147	0.2396
26 to 28	0.0043	0.0474	0.7802
26 to 29	0.0057	0.0625	1.029
28 to 29	0.0014	0.0151	0.249

All the details Given in above table are in per unit system at the base voltage of 345KV(Ph-Ph) and 100MVA . Resistance, impedance and suceptance given are for the total length of transmission lines.

4.3 Transformers

Transformer modelling details [**50**] consists of R_T (Resistance) and X_T (Reactance) which are the equivalent resistance and reactance referred with respect to either the primary or the secondary winding. For this system we assumed that the values are with respect to the primary winding of the transformer. The details of the transformers in IEEE 39 Bus system are given in Table 4.2 below.

Table 4.2 Transformers Data

From Bus	To Bus	Primary Rated Voltage KV	Secondary Rated Voltage KV	Primary Connection Type	Secondary Connection type	Resistance(R_T)	Reactance(X_T)
30	2	20	345	Delta- lag	Star	0.0000	0.0181
37	25	20	345	Delta- lag	Star	0.0006	0.0232
31	6	20	345	Delta- lag	Star	0.0000	0.0250
32	10	20	345	Delta- lag	Star	0.0000	0.0200
11	12	345	345	Star	Star	0.0016	0.0435
13	12	345	345	Star	Star	0.0016	0.0435
34	20	20	345	Delta- lag	Star	0.0009	0.0180
20	19	345	345	Star	Star	0.0007	0.0138
33	19	20	345	Delta- lag	Star	0.0007	0.0142
36	23	20	345	Delta- lag	Star	0.0005	0.0272
35	22	20	345	Delta- lag	Star	0.0000	0.0143
38	29	20	345	Delta- lag	Star	0.0008	0.0156

All the given values are in per unit. For this system, the generator transformers primary winding are delta lag with a rated voltage of 20kV. The secondary windings are star grounded with a rated voltage of 345kV. All the remaining transformers are grounded star-star with the primary and secondary both the windings rated at 345kV.

4.4 Generators

As previously mentioned the IEEE 39 BUS system has 10 generators at different buses. Out of those 10 generators, a generator at BUS31 which is named as GEN2 is assumed to be a slack bus generator. Except for BUS31, all the buses numbered 30 to 39 are referred to as PV buses because of the generators connected at those buses. All the remaining buses are referred to as PQ buses. The bus which is considered as slack bus has a voltage angle defined as zero so that all the remaining voltage angles are measured with respect to the slack generator. The generator

which is considered the slack generator will provide all the deficient power in the network, as well as, gives the power required to cover the losses.

Table 4.3 indicates the initial load flow conditions for the IEEE 39 BUS 10 generators. All the values referred to a 100-MVA power base and at the machines rated terminal voltage.

Table 4.3 Generators Initial Load Flow Details

Bus #	**Generator**	**Rated Voltage kV**	**Voltage Pu**	**Active Power Pu**
30	10	20	1.0475	2.50
31	2	20	0.9820	Slack Generator
32	3	20	0.9831	6.50
33	4	20	0.9972	6.32
34	5	20	1.0123	5.08
35	6	20	1.0493	6.50
36	7	20	1.0635	5.60
37	8	20	1.0278	5.40
38	9	20	1.0265	8.30
39	1	345	1.0300	10.0

Table 4.4 provides the information about the generators rated voltage, inertia, resistance, leakage reactance, transient and sub transient reactance's, and the time constants.

Table 4.4 Generator Details

GEN	**R_a**	**X_l**	**X_d**	**X_q**	**$X_d^{'}$**	**$X_q^{'}$**	**$X_d^{''}$**	**$X_q^{''}$**	**$T_{d0}^{'}$**	**$T_{q0}^{'}$**	**$T_{d0}^{''}$**	**$T_{q0}^{''}$**	**H(S)**
1	0	0.003	0.2	0.019	0.006	0.008	0.0006	0.0006	7	0.7	0.033	0.0563	500
2	0	0.035	0.295	0.282	0.0697	0.17	0.0369	0.0369	6.56	1.5	0.066	0.066	30.3
3	0	0.0304	0.2495	0.237	0.0531	0.0876	0.032	0.032	5.7	1.5	0.057	0.057	35.8
4	0	0.0295	0.262	0.258	0.0436	0.166	0.031	0.031	5.69	1.5	0.057	0.057	28.6
5	0	0.054	0.67	0.62	0.132	0.166	0.0568	0.0568	5.4	0.44	0.054	0.054	26
6	0	0.0224	0.254	0.241	0.05	0.0814	0.0236	0.0236	7.3	0.4	0.073	0.073	34.8
7	0	0.0322	0.295	0.292	0.049	0.186	0.034	0.034	5.66	1.5	0.056	0.056	26.4

Continued…

Table 4.4 Continued

8	0	0.028	0.29	0.28	0.057	0.0911	0.03	0.03	6.7	0.41	0.067	0.067	24.3
9	0	0.0298	0.2106	0.205	0.057	0.0587	0.0314	0.0314	4.79	1.96	0.047	0.047	34.5
10	0	0.0125	0.1	0.069	0.031	0.018	0.0132	0.0132	10.2	0.3	0.1	0.1	42

4.5 Excitation System

Table 4.5 provides the required values to model the excitation system of the generators. All the values are rated with respect to their particular machines ratings. For all the excitation systems, values of the feedback time constant T_f and feedback gain K_f are zeros. Some of the values in the table are assumed values.

Table 4.5 Generators Excitation System Details

GEN	Ex_Tr(s)	Ex_Ka	Ex_ta(s)	Ex_Kp	Ex_Vtmin Pu	Ex_Vtmax Pu	Ex_Vrmin Pu	Ex_Vrmax Pu
1	0.01	125	0.001	5.3	0.1	100	-5.7	12.3
2	0.01	125	0.001	5.3	0.1	100	-5.7	12.3
3	0.01	125	0.001	10	0.1	100	-5.7	12.3
4	0.01	125	0.001	10	0.1	100	-5.7	12.3
5	0.01	125	0.001	20	0.1	100	-5.7	12.3
6	0.01	125	0.001	10	0.1	100	-5.7	12.3
7	0.01	125	0.001	15	0.1	100	-5.7	12.3
8	0.01	125	0.001	15	0.1	100	-5.7	12.3
9	0.01	125	0.001	10	0.1	100	-5.7	12.3
10	0.01	125	0.001	10	0.1	100	-5.7	12.3

4.6 Loads

IEEE 39 BUS system has a total of 19 loads which are connected at different buses. Table 4.6 summarizes the load connected to the respective buses.

Table 4.6 Load Data

BUS	Rated Voltage	Load	Load
3	345	322	2.40
4	345	500	184
7	345	233.8	84.0
8	345	522	176.0
12	345	7.5	88.0
15	345	320	153.0
16	345	329	32.3
18	345	158	30.0
20	345	628	103.0
21	345	274	115.0
23	345	247.5	84.6
24	345	308.6	-92.2
25	345	224	47.2
26	345	139	17.0
27	345	281	75.5
28	345	206	27.6
29	345	283.5	26.9
31	20	9.2	4.6
39	345	1104	250

The next chapter of this dissertation will provide the results including the voltage stability prediction analysis on the test system in Chapter 6 will provide a the summary of this dissertation and purpose future work.

Chapter 5

5 Simulation Results

5.1 Modeling and Dynamic Simulation of IEEE 39 Bus Test System (Phase-I)

To prove the proposed methodology, IEEE 39 bus equivalent test system was built in PSSE (Power System Simulator for Engineering) software to perform dynamic simulations of voltage stable and unstable cases. This research needs detailed modeling information for dynamic simulations, for this reason the IEEE 39 Bus test system equivalent model data was collected from multiple sources. Once the test system was modeled then the load flow solution of the IEEE 39 bus system was verified with those sources.

Phase-I of the methodology discussed earlier in the Section 3.3.1 was to record the system variables like bus voltage magnitudes, voltage angles, generator real and reactive powers, and rotor angles of the system from the dynamic simulations. Once the system models are built, the model will be verified by performing a dynamic simulation for a base case (without applying any contingency) to assure that the dynamic model built in PSSE is stable.

To determine critical contingencies, the test system is stressed by increasing load or disconnecting generating plants or disconnecting transmission lines. Voltage stable and voltage unstable cases were determined for these contingencies. After determining the critical contingencies, dynamic simulations were performed on these cases using the PSSE power system dynamic simulation software. Initially the base case was prepared for dynamic simulations, and then the dynamic simulations were carried out for several cases by applying different contingencies and different loading conditions on the chosen test system and

distinguished the voltage stable and voltage unstable cases by observing the voltage waveforms at all the buses. System parameters or variables such as bus voltage magnitudes, voltage angles, real and reactive powers, and generator rotor angles were extracted from the dynamic simulation data.

The contingency cases used to perform dynamic simulations are summarized in Table 5.1 and this table has the real and reactive power loads connected at the particular mentioned bus, the type of contingency applied and voltage stability for each case.

Table 5.1 Applied Contingencies for the IEEE39 Bus Test System

Case #	Load Bus	P(MW)	Q(MW)	Contingency	Stability
1	4	500	184	Line 4-14	Stable
2	4	600	300	Line 4-14	Stable
3	4	700	400	Line 4-14	Stable
4	4	800	500	Line 4-14	Unstable
5	4	500	184	Line 3-4	Stable
6	4	600	300	Line 3-4	Stable
7	4	700	400	Line 3-4	Unstable
8	4	500	184	Line 4-5	Stable
9	4	600	300	Line 4-5	Stable
10	4	700	400	Line 4-5	Stable
11	4	800	500	Line 4-5	Unstable
12	4	500	184	Line 5-6	Stable
13	4	600	300	Line 5-6	Stable
14	4	700	400	Line 5-6	Stable
15	4	800	500	Line 5-6	Unstable
16	4	500	184	Line 8-9	Stable
17	4	600	300	Line 8-9	Stable
18	4	700	400	Line 8-9	Unstable
19	4	500	184	Line 6-11	Stable
20	4	600	300	Line 6-11	Stable
21	4	700	400	Line 6-11	Stable
22	4	800	500	Line 6-11	Unstable
23	4	500	184	Line 5-8	Stable
24	4	600	300	Line 5-8	Stable
25	4	700	400	Line 5-8	Stable

Continued…

Table 5.1 Continued

Case #	Load Bus	P(MW)	Q(MW)	Contingency	Stability
26	4	800	500	Line 5-8	Unstable
27	4	500	184	Line 6-7	Stable
28	4	600	300	Line 6-7	Stable
29	4	700	400	Line 6-7	Stable
30	4	800	500	Line 6-7	Unstable
31	4	500	184	Line 13-14	Stable
32	4	600	300	Line 13-14	Stable
33	4	700	400	Line 13-14	Stable
34	4	800	500	Line 13-14	Unstable
35	7	500	184	Line 7-8	Stable
36	7	600	300	Line 7-8	Unstable
37	7	500	184	Line 7-6	Stable
38	7	600	300	Line 7-6	Unstable
39	7	500	184	Line 8-9	Unstable
40	7	400	100	Line 8-9	Stable
41	7	500	184	Line 5-8	Stable
42	7	600	300	Line 5-8	Unstable
43	7	500	184	Line 4_14	Stable
44	7	600	300	Line 4_14	Unstable
45	7	500	184	Line 3-4	Unstable
46	7	400	100	Line 3-4	Stable
47	7	500	184	Line 4-5	Stable
48	7	600	300	Line 4-5	Unstable
49	7	500	184	Line 5-6	Stable
50	7	600	300	Line 5-6	Unstable
51	7	500	184	Line 6-11	Stable
52	7	600	300	Line 6-11	Unstable
53	7	500	184	Line 6-31	Stable
54	7	600	300	Line 6-31	Unstable
55	7	500	184	Line 10-11	Stable
56	7	600	300	Line 10-11	Unstable
57	7	500	184	Line 10-32	Unstable
58	7	400	100	Line 10-32	Unstable
59	7	300	50	Line 10-32	Stable
60	8	500	184	Line 8-9	Stable
61	8	600	300	Line 8-9	Stable
62	8	700	400	Line 8-9	Unstable
63	8	500	184	Line 8-5	Stable
64	8	600	300	Line 8-5	Stable
65	8	700	400	Line 8-5	Stable
66	8	800	500	Line 8-5	Unstable
67	8	500	184	Line 8-7	Stable

Continued…

Table 5.1 Continued

Case #	Load Bus	P(MW)	Q(MW)	Contingency	Stability
68	8	600	300	Line 8-7	Stable
69	8	700	400	Line 8-7	Stable
70	8	800	500	Line 8-7	Unstable
71	8	500	184	Line 4-5	Stable
72	8	600	300	Line 4-5	Stable
73	8	700	400	Line 4-5	Stable
74	8	800	500	Line 4-5	Unstable
75	8	500	184	Line 6-7	Stable
76	8	600	300	Line 6-7	Stable
77	8	700	400	Line 6-7	Stable
78	8	800	500	Line 6-7	Unstable
79	8	500	184	Line 6-11	Stable
80	8	600	300	Line 6-11	Stable
81	8	700	400	Line 6-11	Unstable
82	8	500	184	Line 4-14	Stable
83	8	600	300	Line 4-14	Stable
84	8	700	400	Line 4-14	Stable
85	8	800	500	Line 4-14	Unstable
86	8	500	184	Line 3-4	Stable
87	8	600	300	Line 3-4	Stable
88	8	700	400	Line 3-4	Unstable
89	8	500	184	Line 5-6	Stable
90	8	600	300	Line 5-6	Stable
91	8	700	400	Line 5-6	Stable
92	8	800	500	Line 5-6	Unstable
93	8	500	184	Line 6-31	Stable
94	8	600	300	Line 6-31	Stable
95	8	700	400	Line 6-31	Unstable
96	18	158	30	Line 18-3	Stable
97	18	260	130	Line 18-3	Stable
98	18	360	230	Line 18-3	Stable
99	18	560	330	Line 18-3	Unstable
100	18	158	30	Line 3-2	Stable
101	18	260	130	Line 3-2	Stable
102	18	360	230	Line 3-2	Stable
103	18	460	330	Line 3-2	Unstable
104	18	158	30	Line 18-17	Stable
105	18	260	130	Line 18-17	Stable
106	18	360	230	Line 18-17	Stable
107	18	460	330	Line 18-17	Unstable
108	18	158	30	Line 2-25	Stable
109	18	260	130	Line 2-25	Stable

Continued…

Table 5.1 Continued

Case #	Load Bus	P(MW)	Q(MW)	Contingency	Stability
110	18	360	230	Line 2-25	Stable
111	18	460	330	Line 2-25	Unstable
112	18	158	30	Line 3-4	Stable
113	18	260	130	Line 3-4	Stable
114	18	360	230	Line 3-4	Stable
115	18	460	330	Line 3-4	Unstable
116	3	322	2.4	Line 2-3	Stable
117	3	420	100	Line 2-3	Stable
118	3	520	200	Line 2-3	Stable
119	3	620	300	Line 2-3	Unstable
120	3	322	2.4	Line 3-18	Stable
121	3	420	100	Line 3-18	Stable
122	3	520	200	Line 3-18	Stable
123	3	620	300	Line 3-18	Unstable
124	3	322	2.4	Line 3-4	Stable
125	3	420	100	Line 3-4	Stable
126	3	520	200	Line 3-4	Stable
127	3	620	300	Line 3-4	Unstable
128	3	322	2.4	Line 17-18	Stable
129	3	420	100	Line 17-18	Stable
130	3	520	200	Line 17-18	Stable
131	3	620	300	Line 17-18	Unstable
132	3	322	2.4	Line 2-25	Stable
133	3	420	100	Line 2-25	Stable
134	3	520	200	Line 2-25	Stable
135	3	620	300	Line 2-25	Unstable
136	3	322	2.4	Line 3-2	Stable
137	3	552	232.4	Line 3-2	Stable
138	3	555	257.4	Line 3-2	Unstable
139	3	322	2.4	Line 3-4	Stable
140	3	602	282.4	Line 3-4	Stable
141	3	607	287.4	Line 3-4	Unstable
142	3	322	2.4	Line 5-6	Stable
143	3	607	287.4	Line 5-6	Stable
144	3	610	290.4	Line 5-6	Unstable
145	3	322	2.4	Line 3-18	Stable
146	3	605	285.4	Line 3-18	Stable
147	3	610	290.4	Line 3-18	Unstable
148	3	322	2.4	Line 2-25	Stable
149	3	605	285.4	Line 2-25	Stable
150	3	610	290.4	Line 2-25	Unstable
151	3	322	2.4	Line 4-14	Stable

Continued…

Table 5.1 Continued

Case #	Load Bus	P(MW)	Q(MW)	Contingency	Stability
152	3	605	285.4	Line 4-14	Stable
153	3	610	290.4	Line 4-14	Unstable
154	4	500	184	Line 4-14	Stable
155	4	740	424	Line 4-14	Stable
156	4	750	434	Line 4-14	Unstable
157	4	500	184	Line 3-4	Stable
158	4	660	344	Line 3-4	Stable
159	4	670	354	Line 3-4	Unstable
160	4	500	184	Line 4-5	Stable
161	4	760	444	Line 4-5	Stable
162	4	770	454	Line 4-5	Unstable
163	4	500	184	Line 5-6	Stable
164	4	750	434	Line 5-6	Stable
165	4	760	444	Line 5-6	Unstable
166	4	500	184	Line 8-9	Stable
167	4	660	344	Line 8-9	Stable
168	4	670	354	Line 8-9	Unstable
169	4	500	184	Line 6-11	Stable
170	4	730	414	Line 6-11	Stable
171	4	740	424	Line 6-11	Unstable
172	4	500	184	Line 5-8	Stable
173	4	750	434	Line 5-8	Stable
174	4	760	444	Line 5-8	Unstable
175	4	500	184	Line 6-7	Stable
176	4	750	434	Line 6-7	Stable
177	4	760	444	Line 6-7	Unstable
178	4	500	184	Line 13-14	Stable
179	4	730	414	Line 13-14	Stable
180	4	740	424	Line 13-14	Unstable
181	8	522	176	Line 8-5	Stable
182	8	772	426	Line 8-5	Stable
183	8	782	436	Line 8-5	Unstable
184	8	522	176	Line 8-7	Stable
185	8	782	436	Line 8-7	Stable
186	8	792	446	Line 8-7	Unstable
187	8	522	176	Line 8-9	Stable
188	8	662	316	Line 8-9	Stable
189	8	672	326	Line 8-9	Unstable
190	8	522	176	Line 4-5	Stable
191	8	732	386	Line 4-5	Stable
192	8	742	396	Line 4-5	Unstable
193	8	522	176	Line 6-7	Stable

Continued…

Table 5.1 Continued

Case #	Load Bus	P(MW)	Q(MW)	Contingency	Stability
194	8	782	436	Line 6-7	Stable
195	8	792	446	Line 6-7	Unstable
196	8	522	176	Line 6-11	Stable
197	8	692	346	Line 6-11	Stable
198	8	702	356	Line 6-11	Unstable
199	8	522	176	Line 4-14	Stable
200	8	782	436	Line 4-14	Stable
201	8	792	446	Line 4-14	Unstable
202	8	522	176	Line 3-4	Stable
203	8	672	326	Line 3-4	Stable
204	8	682	336	Line 3-4	Unstable
205	8	522	176	Line 5-6	Stable
206	8	752	406	Line 5-6	Stable
207	8	762	416	Line 5-6	Unstable
208	8	522	176	Line 6-31	Stable
209	8	672	326	Line 6-31	Stable
210	8	682	336	Line 6-31	Unstable
211	12	8,5	88	Line 12-11	Stable
212	12	248.5	328	Line 12-11	Stable
213	12	258.5	338	Line 12-11	Unstable
214	12	8.5	88	Line 12-13	Stable
215	12	278.5	358	Line 12-13	Stable
216	12	288.5	368	Line 12-13	Unstable
217	12	8.5	88	Line 10-11	Stable
218	12	208.5	288	Line 10-11	Stable
219	12	218.5	298	Line 10-11	Unstable
210	12	8.5	88	Line 10-13	Stable
211	12	238.5	318	Line 10-13	Stable
212	12	248.5	328	Line 10-13	Unstable
213	12	8.5	88	Line 6-31	Stable
214	12	138.5	218	Line 6-31	Stable
215	12	148.5	228	Line 6-31	Unstable
216	12	8.5	88	Line 6-11	Stable
217	12	248.5	328	Line 6-11	Stable
218	12	258.5	338	Line 6-11	Unstable
219	12	8.5	88	Line 13-14	Stable
220	12	208.8	288,3	Line 13-14	Stable
221	12	218.5	298	Line 13-14	Unstable

As mentioned earlier in this document, this research doesn't consider or investigate the reasons behind the voltage collapse. For readers better understanding of voltage collapse a stable and an unstable case was selected, and the reason behind voltage collapse is explained in this section.

The waveform of Bus 7 voltage for case 40 is presented in Figure 5.1 and Figure 5.2. Transmission line between Bus 8 and Bus 9 was disconnected at 10 seconds. Now the power required by load 8 has to be supplied by SM2 and SM3 through the transmission line L7_8. This causes voltage drop at the terminal buses of the machines SM2 and SM3.When the line was disconnected, voltage at Bus 7 drops from 0.94 p.u to 0.91 p.u. The time constant for all the ULTCs (Under load tap changers) is 20 seconds. Around 32 seconds ULTC3 near the synchronous machine SM2 operates and try to increase the voltage at the buses close to SM2 especially at Bus 6 where the ULTC3 was connected. At 50 seconds ULTC near the machine SM3 operates and increases the voltage at Bus 10 where ULTC4 was connected. This intern increases the voltage at the Bus 6, Bus 7 and Bus 8. These two ULTCS will bring the voltage at Bus 6 and Bus 10 to their pre-fault voltages, but Bus 8 voltage was not came back to its pre-fault voltage because the power required by Load 8 is now solely supplied by L7_8 which will lead to more voltage drop in the transmission line. The post fault voltage is settled at 0.93 p.u. By looking at the Bus 7 voltage will confirm that the system is voltage stable. This can be observed in below figures.

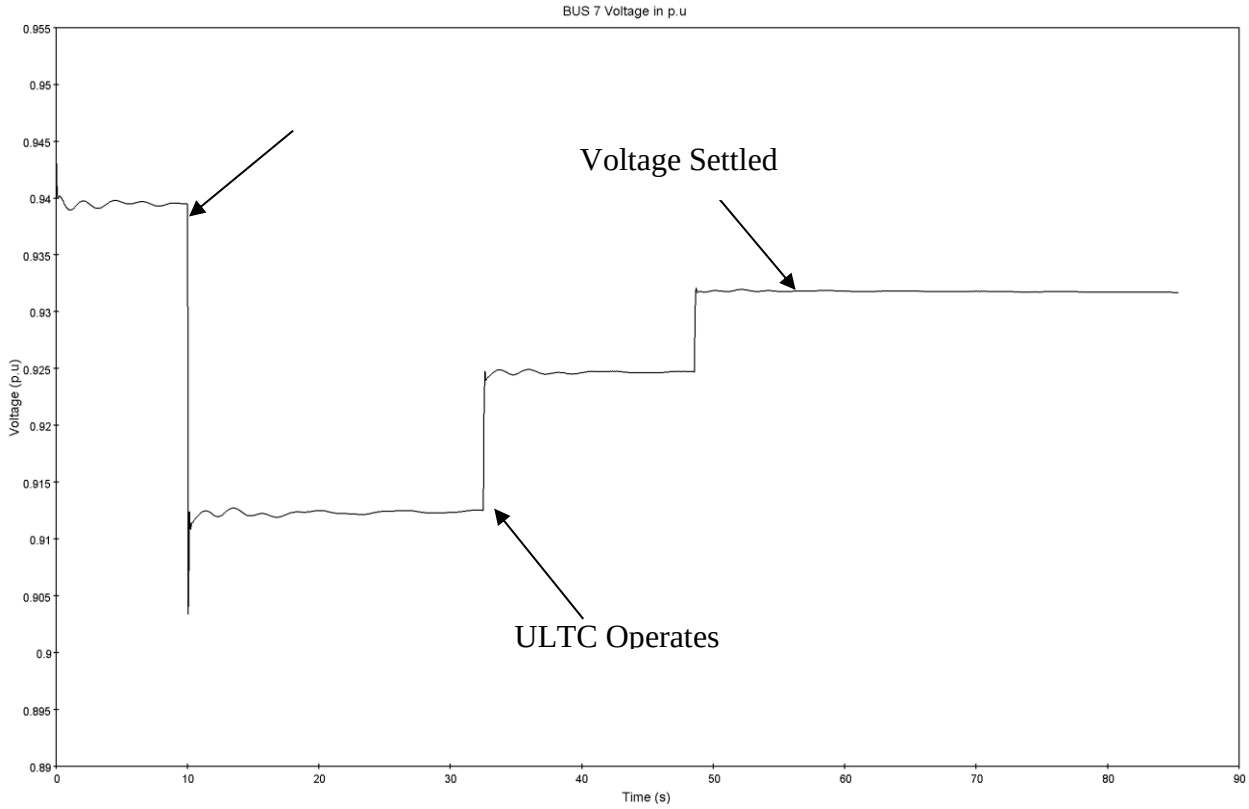

Figure 5.1 Bus 7 Voltage for Stable Case 40

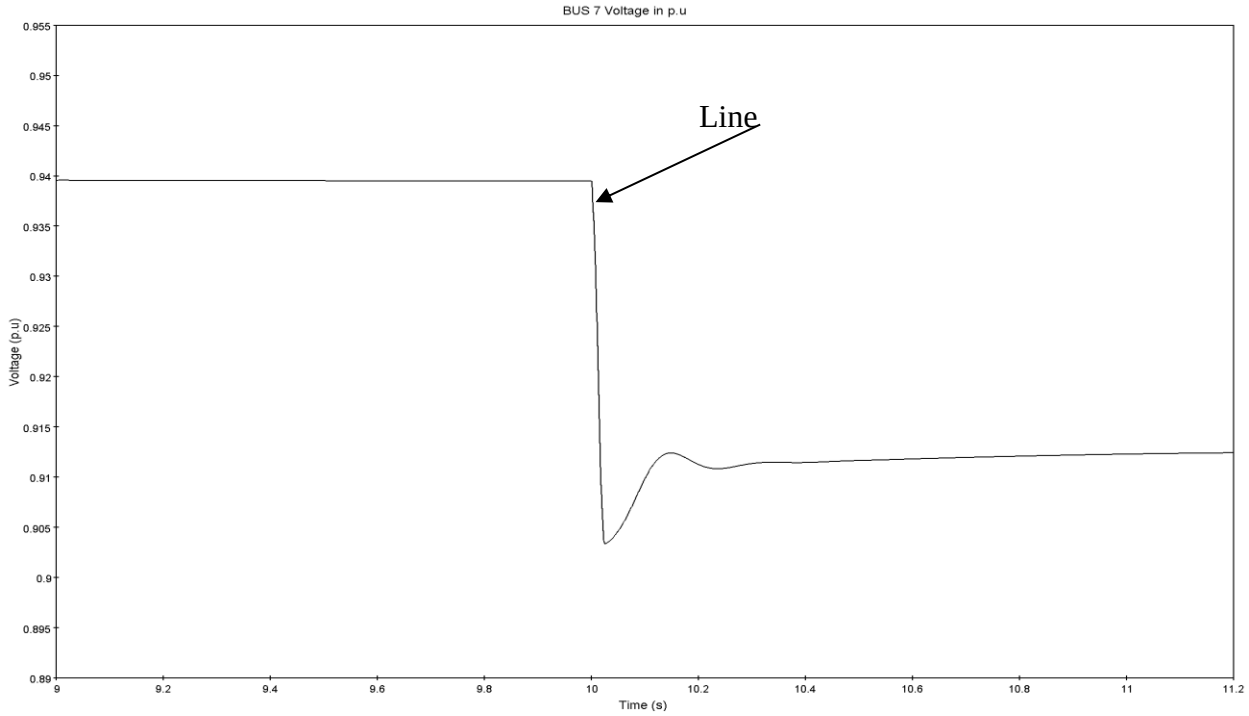

Figure 5.2 Zoomed in Figure 5.1

Figure 5.3 and Figure 5.4 illustrates the simulation result for an outage of transmission line at 10 seconds between Bus 8 and Bus 9 for case 39 loading. Power required by load 8 has to be supplied by SM2 and SM3 through the transmission line L7_8. This causes voltage drop at the terminal buses of the machines SM2 and SM3. After the tripping of transmission line reactive power required by load at Bus 8 is taking power from SM2 and SM3 which is given by over exciting the synchronous machines. Time constant of VOX (Over Excitation limiter) is set to 20 seconds. These over excitation limiters will try to control the excitation current to synchronous machines. This causes SM2 and SM3 to deliver constant reactive power because reactive power and voltage are relative to each other. This means supplying more reactive power to load is achieved by increasing the excitation current which will increase the terminal voltage of synchronous machines. But when ULTC detects an under voltage, it will try to increase the

voltage on the secondary of the transformer by changing the tap position. This will decrease the voltage on the primary side of transformer which is connected to the synchronous machines terminal Bus. Then generators cannot give enough reactive power to load. The net effect of each tap movement of ULTC is to reduce the secondary voltage rather than increase. The combined action of VOX and ULTC will lead to voltage collapse and it is shown in below figure.

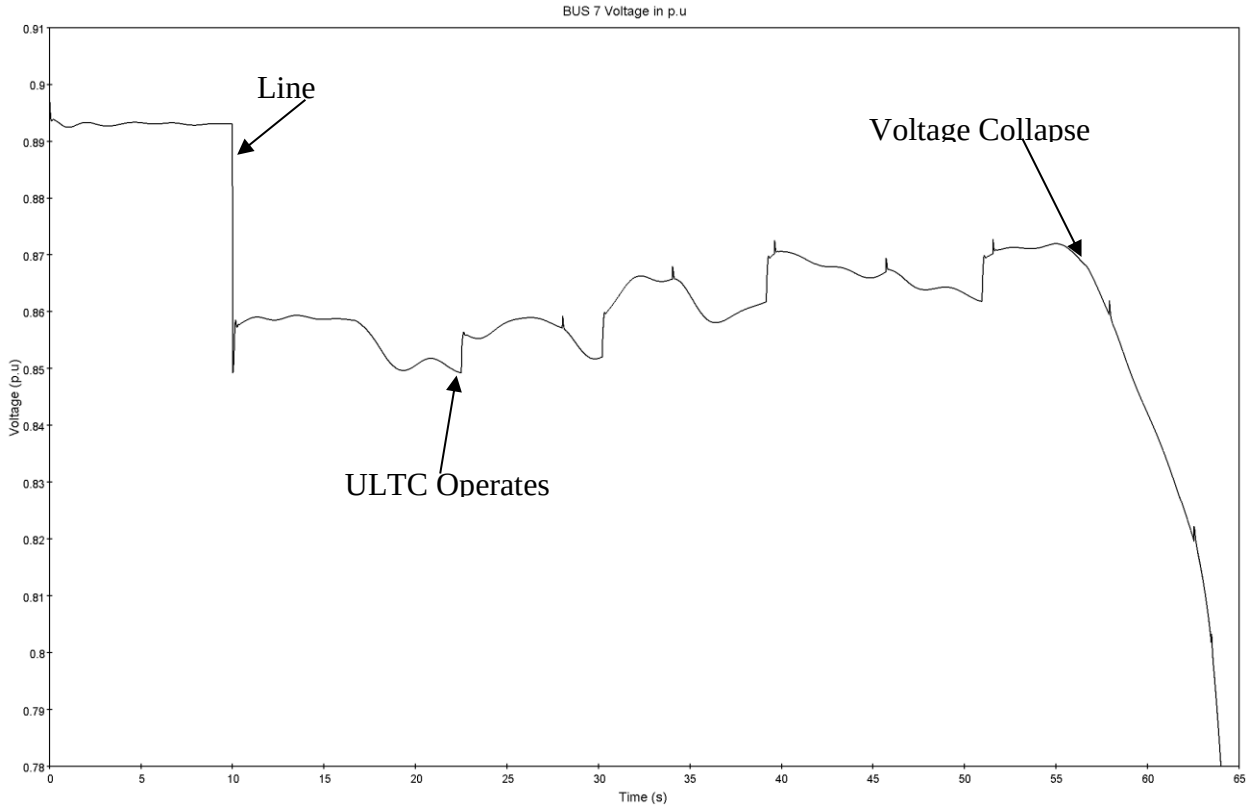

Figure 5.3 Bus 7 Voltage for Unstable Case 39

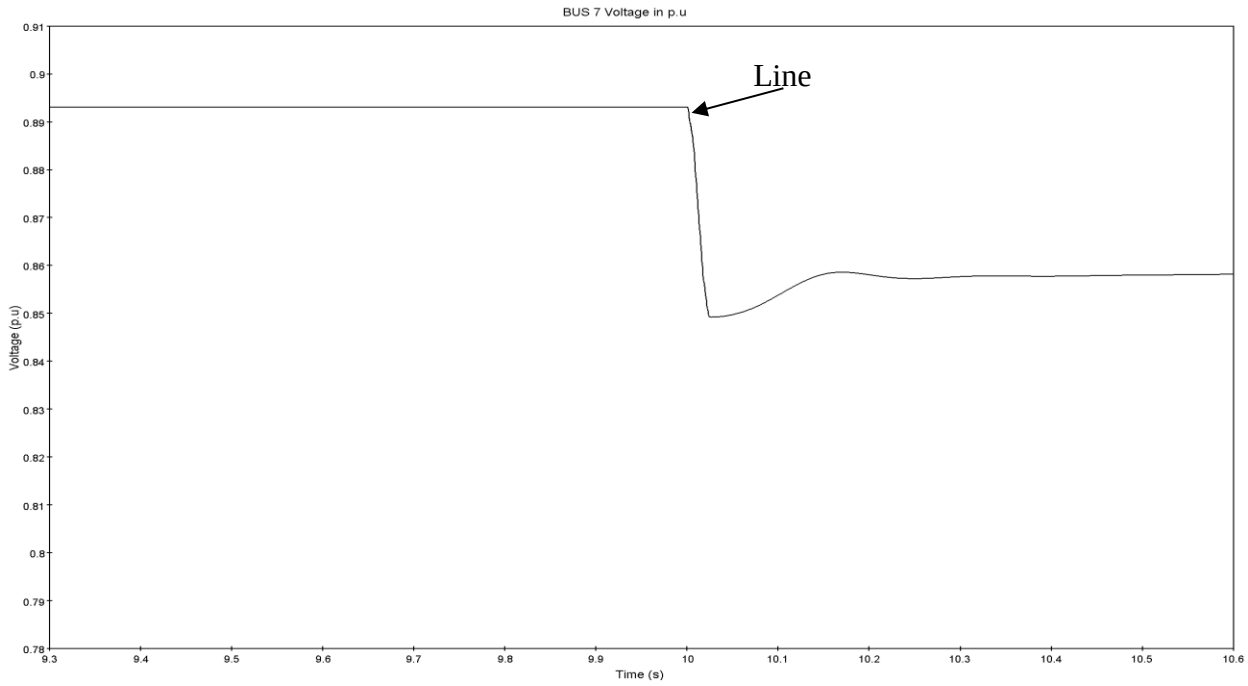

Figure 5.4 Zoomed in Figure 5.3

Time domain dynamic simulation data around the contingency between 10 to 15 seconds are studied to distinguish voltage stability problem from the system dynamics. This data includes the disconnecting of the transmission line at 10^{th} second and the dynamics after disconnecting the transmission line. This research will prove that this data is sufficient to detect voltage stability from system dynamics.

5.2 Data Processing and Feature Extraction

The previous section has provided an insight in to the test system modeling, contingency analysis, and dynamic simulations. As of this point this research has performed dynamic simulations and has the system parameters like bus voltage magnitudes and angles, generator real and reactive power dispatches, and transmission line power flows extracted for all the cases.

Now this section will cover data processing and feature extraction part of the proposed methodology. This research utilizes MATLAB to process the data obtained from PSSE dynamic simulation to build the features in the given time window.

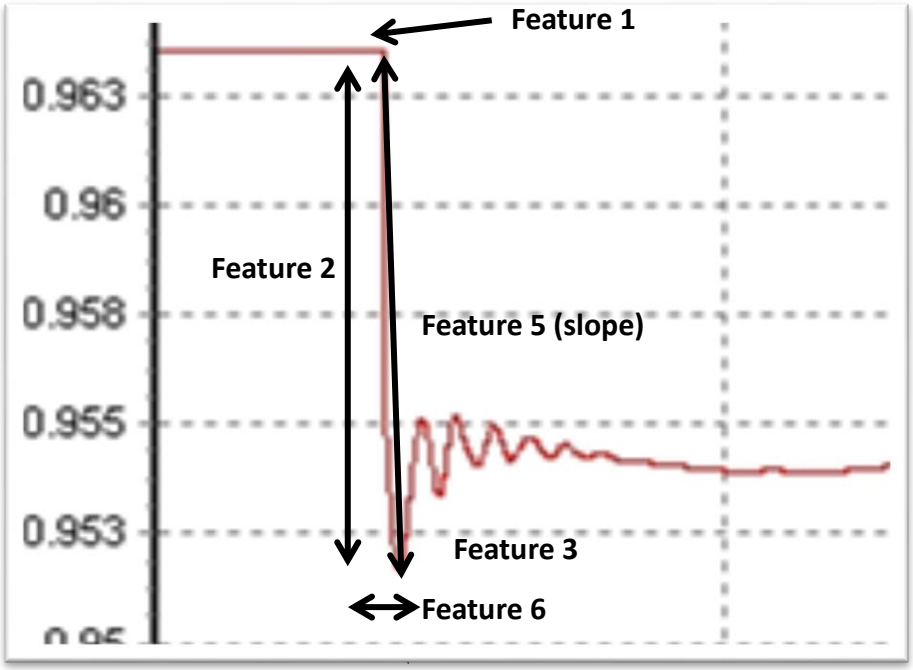

Figure 5.5 Feature 1, Feature 2, and Feature 3

Figure 5.5 shows the feature extraction from system parameters of our interest as mentioned earlier from the time domain dynamic simulations.

- Feature 1 is the value of system parameter before the contingency.
- Feature 2 is the magnitude of the drop right after the contingency at 10 seconds of the simulation.
- Feature 3 is the immediate rise of the system parameter following the first drop.
- Feature 4 is the ratio of the drop (Column 2) and rise (column 3).

- Feature 5 is the slope of the drop after the contingency.
- Feature 6 is the time system dynamics took for the first oscillations.
- Feature 7 is system parameter average for first five seconds of the dynamics immediately following the contingency.
- Feature 8 is the system parameter standard deviation for first five seconds of the dynamics immediately following the contingency.
- Feature 9 is the system parameter median for first five seconds of the dynamics immediately following the contingency.
- Feature 10 is the immediate value of the system parameter after contingency.

Table 5.2 gives all the features collected from the system parameters- bus voltage magnitudes and angles, generator real and reactive power dispatches, and transmission line power flows for all the elements in IEEE39 Bus test system.

Table 5.2 Features Extracted From System Parameters

System Parameter	Number of Elements	Fea1	Fea2	Fea3	Fea4	Fea5	Fea6	Fea7	Fea8	Fea9	Fea10	Total Features
Bus Voltage Magnitude	39 Buses	●	●	●	●	●	●	●	●	●	○	351
Bus Voltage Angle	39 Buses	●	●	●	●	●	●	●	●	●	○	351
Gen Rotor Angle	10 Generators	●	●	●	●	●	●	●	●	●	○	90
Gen Real Power	10 Generators	●	●	●	●	●	●	●	●	●	●	100
Gen Reactive Power	10 Generators	●	●	●	●	●	●	●	●	●	●	100
Branch Real Power Flow	92 Branches	●	○	○	○	○	○	○	○	○	○	92

Continued…

Table 5.2 Continued

System Parameter	Number of Elements	Fea1	Fea2	Fea3	Fea4	Fea5	Fea6	Fea7	Fea8	Fea9	Fea10	Total Features
Branch Reactive Power Flow	92 Branches	●	○	○	○	○	○	○	○	○	○	92
Branch MVA Flow	92 Branches	●	○	○	○	○	○	○	○	○	○	92

Total 1268 features or data points were extracted from the system parameters for the dynamic simulations performed on each case described in Table 5.1. To train and to test the proposed methodology in detecting voltage abnormality, the 221 dynamic simulations of stable and unstable cases have been categorized into 120 sets of training cases and 101 test cases. Out of these 120 training cases, 84 cases were voltage stable cases and the remaining 36 cases were voltage unstable cases and these cases were used to train the pattern recognition methods. The 101 cases chosen for the purpose of testing the trained pattern recognition technique has 72 stable cases and 29 unstable cases.

5.3 Prediction of Voltage Abnormality Using Proposed Methodology

Salford System's data mining software CART® was used and the 120 training sets created earlier were used to build CART trees. This research utilized Gini indexing. Linear Combinations (LC) option was used in the analysis. Linear combination means all possible mathematical combinations of the variables or predictors. Instead of using a single variable for splitting a node, a linear combination of one or more predictors is used. CART goes through the training set of 120 cases and applies the linear combination to the features of 1268 dimension. After the linear combination analysis, CART comes up with a classification tree topology with the minimum possible relative cost. Figure 5.6 presents the relative cost for different tree

topologies and it will also confirms that the most efficient tree with the minimum relative cost has three nodes.

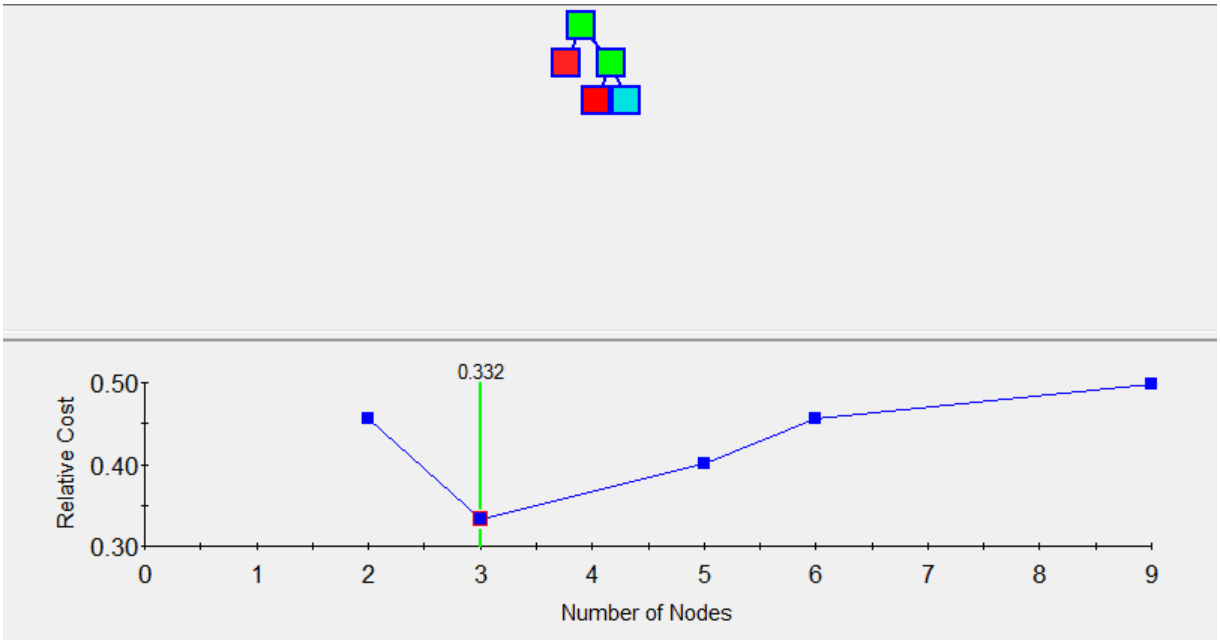

Figure 5.6 Relative Cost for the Classification Tree Topology

The CART tree obtained from the training set is shown in Figure 5.7. Out of 1268 features from each dynamic simulation, CART determined COL43 (Feature 7 of Table 5.2 of Bus 5 voltage magnitude average for first five seconds of the dynamics immediately following the contingency) as the root node. CART has also determined COL127 (Feature 1 of Table 5.2 of Bus 15 voltage magnitude just before the contingency) as child node. CART has determined that the Bus voltage magnitudes at BUS 5 and BUS 15 as the prominent features in detecting the voltage abnormality for the IEEE 39 bus test system. Figure 5.7 confirms that, if Col5 of Bus 5 voltage magnitude is greater than 0.96 is classified as voltage stable. If Col5 of Bus 5 voltage magnitude is less than 0.96, and Col5 of Bus 5 voltage magnitude is greater than 0.96 and Col1 of Bus 15 voltage magnitude less than 0.99 as voltage unstable case.

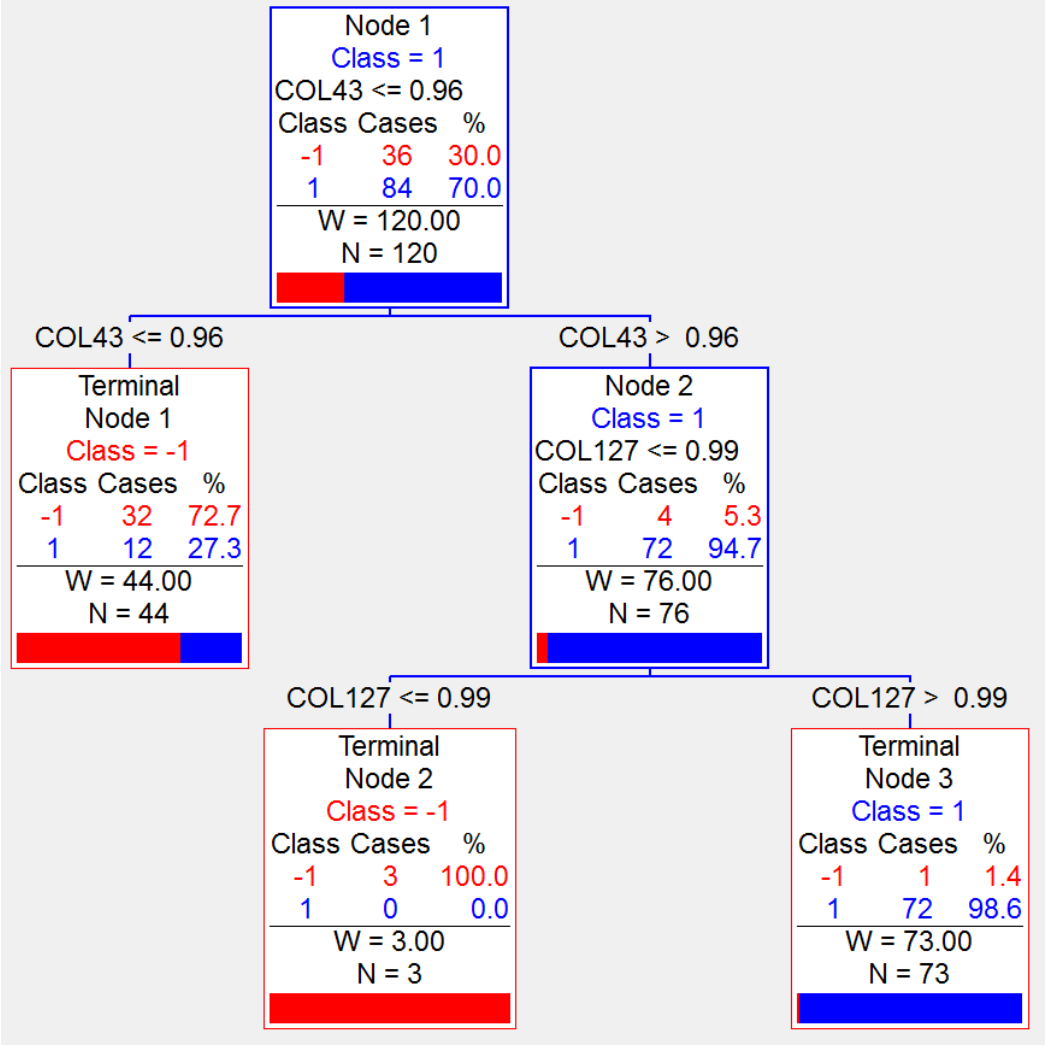

Figure 5.7 CART Tree Grooved for the Training Set

After generating the CART trees (Groove file- trained pattern recognition algorithm) from the training sets, test sets were inputted to the groove file and CART has determined voltage stable cases and voltage unstable cases.

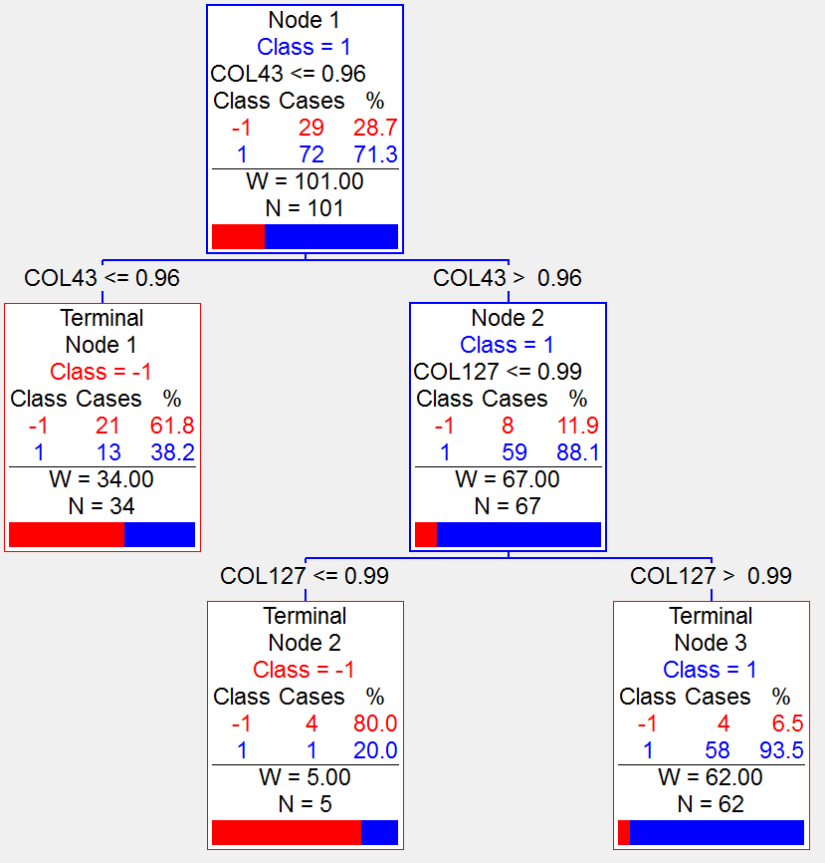

Figure 5.8 CART Tree for the Test Set

Figure 5.8 shows the CART tree formed for the test set. Out of 72 stable cases, 58 cases were classified as stable and the remaining 14 cases as unstable cases. Out of 29 unstable cases, 25 were classified as unstable cases and 4 as stable cases.

Table 5.3 Accuracy of CART on Training Sets

Type of Simulation Case	**Classified as Stable**	**Classified as Unstable**	**Accuracy (%)**
Stable (84)	72	12	85.71
Unstable (36)	1	35	97.22

Table 5.4 Accuracy of CART on Test Sets

Type of Simulation Case	**Classified as Stable**	**Classified as Unstable**	**Accuracy (%)**
Stable (72)	58	14	80.55
Unstable (29)	4	25	86.20

Table 5.3 and Table 5.4 provide the accuracy of the CART pattern recognition technique for the training and test data sets. It is this research main intention to predict the voltage unstable cases, and by misclassifying a stable case as unstable case has little effect as compared to classifying an unstable case as stable case.

The 1268 features or data points extracted from the system parameters from the dynamic simulations performed on the 120 training cases were used to train the RLSC algorithm. The algorithm described earlier in last section was developed in MATLAB environment. The regularization parameter $\lambda > 0$ in Equation 3.3 is not known a-priori and has to be determined based on the problem data. The training data was used to train the LASSO RLSC pattern recognition method for different Lambda values. The use of LASSO regularization model reduced the number of predictors in the estimation model and this provided the important features in predicting the voltage collapse.

The plot showed in Figure 5.9 shows the nonzero coefficients in the regression for various values of the Lambda regularization parameter. Larger values of Lambda appear on the left side of the graph, meaning more regularization, resulting in fewer nonzero regression

coefficients. The upper part of the plot shows the degrees of freedom (df), meaning the number of nonzero coefficients in the regression, as a function of Lambda. On the left, the large value of Lambda causes all but one coefficient to be 0. On the right 206 coefficients out of 1268 predictors are nonzero.

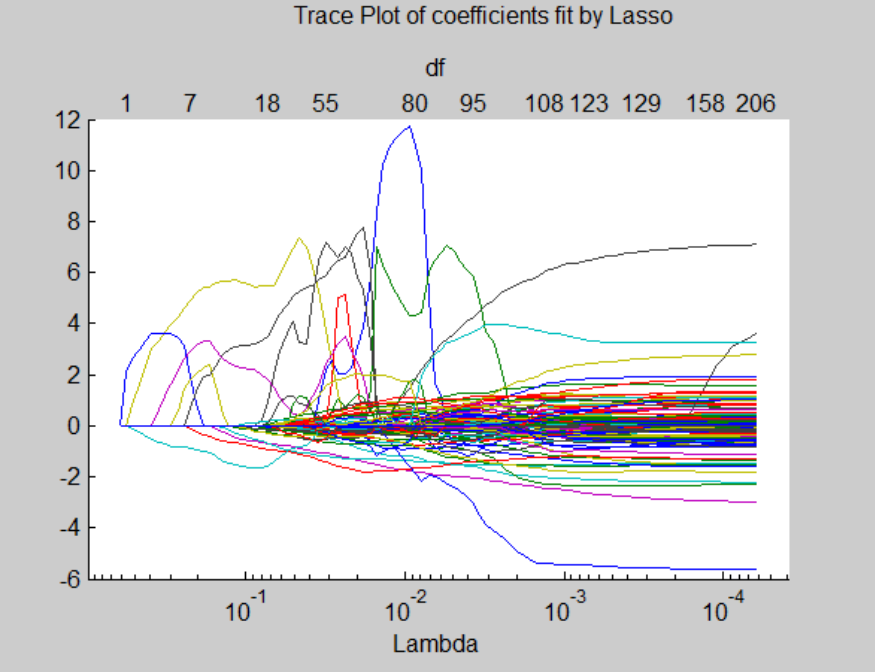

Figure 5.9 LASSO Plot of Lagrange multiplier λ Versus Predictor Equation Coefficients C_i

Once the RLSC algorithm was trained, the 101 test cases were supplied to test the accuracy of the algorithm for all the Lambda values considered to train LASSO pattern recognition algorithm. Table 1 summarizes the accuracy of the pattern recognition technique in detecting voltage collapse for five different lambda values and the number of non-zero coefficients for the function f(x).

Table 5.5 Accuracy of RLSC Pattern Recognition Method for Different λ Values

λ	Accuracy(%)	Number of non zero coefficients
0.2235	83.16	7
0.1691	82.17	6
0.2954	81.18	4
0.2453	80.19	6
0.2692	79.20	5

From the Table 5.5 this research can conclude that for the chosen IEEE 39 bus test system the optimistic λ value is 0.2235 and the number of non-zero coefficients is 7. This means to determine the voltage stability of the IEEE 39 bus test system only requires 7 parameters out of 1268 features collected from the test system dynamic variables. These 7 parameters are the prominent features needed to predict the voltage collapse. Table 5.6 will summarize all these seven prominent features used in the voltage stability prediction for the test system.

Table 5.6 Prominent Features from RLSC

System Parameter	Feature
Bus 4 Voltage Magnitude	Feature 7
Bus 5 Voltage Magnitude	Feature 7
Bus 8 Volatge Magnitude	Feature 1
Bus 10 Voltage Magnitude	Feature 7
Bus 14 Volatge Magnitude	Feature 7
Generator 2 Reactive Power	Feature 4
Generator 10 Reactive power	Feature 2

Once the RLSC algorithm was trained, the 101 test cases were supplied to test the accuracy of the algorithm. This trained algorithm was also tested on training set used to train the RLSC algorithm. Table 5.7 and

Table 5.8 gives the accuracy of the RLSC algorithm for the training set and test set.

Table 5.7 Accuracy of RLSC on Training Sets

Type of Simulation Case	**Classified as Stable**	**Classified as Unstable**	**Accuracy (%)**
Stable (84)	81	3	96.42
Unstable (36)	15	21	58.33

Table 5.8 Accuracy of RLSC on Test Sets

Type of Simulation Case	**Classified as Stable**	**Classified as Unstable**	**Accuracy (%)**
Stable (72)	68	4	94.44
Unstable (29)	13	16	55.17

Table 5.9 and Table 5.10 provide the accuracy of the CART and RLSC pattern recognition technique for all the dynamic simulations cases given in table 5.1. By observing the accuracies of RLSC for stable cases and CART for unstable cases, this research concludes that RLSC is a promising patter recognition method for detecting voltage stable cases and CART is accurate in predicting voltage unstable cases.

Table 5.9 Accuracy of CART Pattern Recognition Method

Type of Simulation Case	**Classified as Stable**	**Classified as Unstable**	**Accuracy (%)**
Stable (156)	130	26	83.33
Unstable (65)	5	60	92.30

Table 5.10 Accuracy of RLSC Pattern Recognition Method

Type of Simulation Case	**Classified as Stable**	**Classified as Unstable**	**Accuracy (%)**
Stable (156)	148	8	94.87
Unstable (65)	20	45	69.23

The methodology proposed in this research will suggest assigning weights for each of the pattern recognition methods depending on their end results. For an unstable case the combined algorithm will put higher weight for CART than RLSC, this means if CART says unstable and RLSC classifies it as stable the end result will be a voltage unstable case. This decision making will aid the proposed methodology in detecting voltage collapse, because classifying a stable case as unstable case has lower impact than classifying a voltage unstable case as a stable case. By taking remedial actions for a misclassified stable case will have less impact than not taking remedial actions for an unstable phenomenon.

The main intention of the proposed methodology is to predict voltage collapse long before it happens and because of this reason this research recommends to use CART to predict the voltage collapse.

As proven in this section, the proposed methodology only needs Bus 5 and Bus 15 voltage magnitudes immediately following the disturbance for the IEEE39 bus test system to predict the voltage collapse. By observing the IEEE 39 bus system topology given in Figure 4.1, the Bus 5 and Bus 15 serves for the purpose of transporting power from the generating stations to the different load centers and observing these bus voltage magnitudes at these buses will provide a good measure of voltage stability. These findings will also encourage the proposed methodology to be used for online voltage stability analysis because once the prominent features are determined; one only needs to monitor those for the prediction of voltage stability.

Chapter 6

6 Summary and Future Work

6.1 Summary

The dissertation presents a method to detect voltage stability of a power system in its earlier stages by analyzing the dynamic behavior of the stressed power system. To correlate dynamic behavior to system voltage abnormality, this research utilized pattern recognition methods such as algorithmic Regularized Least Square Classification (RLSC) pattern recognition or a statistical method such as Classification and Regression Tree (CART). This research used PSSE to simulate the stressed system and used RLSC and CART to predict system voltage abnormality in future. To capture the dynamics of stressed system, this research introduced numerous contingencies and driven the system to the point of abnormal operation and then identified those simulated contingencies that cause system voltage abnormality.

Chapter 1 of this dissertation report gave an introduction on power system stability and its classification on different basis. This chapter has also gave a brief introduction of voltage stability and its problems. Voltage stability analysis methods and a review on voltage stability were discussed. Literature reviews of voltage stability analysis methods were presented. Especially static methods of voltage stability analysis and dynamic methods of voltage stability analysis were compared and advantages and disadvantages were discussed. Some case studies were included on the major blackouts occurred throughout the world, and the main reasons for the blackouts were also given in the case studies.

The concepts, definitions and methods required to study the voltage stability are presented in Chapter 2 of this report. This part of the report covers the existing static and dynamic voltage stability analysis methods. The advantages and disadvantages of the voltage stability analysis methods were discussed. This section gave a perspective of power system dynamics and their mathematical models. A small four bus power system with synchronous generators, transmission lines, induction motors and capacitor banks was used to demonstrate the various system dynamics with respect to their operating time span. Instantaneous, short-term, and long-term dynamics with their respective mathematical models for the power system were also presented in this chapter. The techniques to separate, simplify the dynamic models of a power system was discussed. Application of time-scale decomposition to the power systems was also explained in Chapter 2

The difficulties in detecting voltage collapse were reviewed and explained in Chapter 3 of this report. This chapter demonstrated the objective of this research to detect voltage collapse by analyzing dynamic behavior of a stressed power system and to correlate the dynamic responses to the future system voltage abnormality. The methodology used to achieve the objective was discussed in detail with the help of flowcharts in this section. The three phases involved in achieving the objective were also presented. The concepts and principles of pattern recognition were introduced. Chapter 3 also discussed the methodology in applying pattern recognition techniques to detect the voltage collapse by observing the dynamic behavior of the power systems.

Chapter 4 has provided the data needed to model the IEEE 39 bus test system in PSSE power system simulator tool. This chapter also covered some basics needed to understand the modeling of the power system to perform dynamic simulations.

The results of the dynamic simulations of the IEEE 39 bus test system and the system voltage stability for those simulations were presented in Chapter 5 of this dissertation report. A case study for a voltage stable and voltage unstable case was provided to give the better understanding of the system dynamics role in the voltage stability. The voltage stable and voltage unstable dynamic simulation cases were split into training and test set cases to prove the proposed methodology. CART and RLSC pattern recognition algorithms were trained using the training set and the trained algorithm was tested using the test set of the dynamic simulations. After the pattern recognition analysis on the dynamic simulations the research has concluded that CART is accurate in predicting voltage unstable cases and RLSC is accurate in predicting voltage stable cases. This chapter also presented the prominent features to detect the voltage collapse for the IEEE 39 bus test system and suggested to use those features for online voltage stability analysis.

6.2 Future Work

Although the analysis and validation of the methodology is performed using the IEEE 39 Bus system, it is our intention in future to apply the proposed method to a real size power systems by using raw system response captured by phasor measurement units (PMU) installed at certain location of electric utilities. By collecting data from PMUs and training the pattern recognition models to recognize historical abnormal events, the methodology will be useful in assessing online voltage stability of power systems and identifying patterns that lead to voltage

abnormalities ahead of time for use by operators in applying remedial actions for possible prevention of blackouts. In this dissertation we only have looked at two different pattern recognition techniques but in future we want to investigate different pattern recognition techniques.

7 Bibliography

[1] P. Kundur, *Power system voltage stability and control*. New York: Mc-Graw Hill, 1994.

[2] C. W. Taylor, *Power system voltage stability*. New York, USA: McGraw-Hill, 1994.

[3] Y. Tamura, "Relationship between voltage instability and multiple load flow solutions in electric power system," *IEEE Trans. on PAS*, vol. PAS-102, pp. 1115-1125, May 1983.

[4] F. D. Galiana, "Load flow feasibility and the voltage collapse problem," in *IEEE Proceedings of 23rd Conference on Control and Decision*, Las Vegas, Dec 1984, pp. 485-487.

[5] M. Brucoli, "A generalized approach to the analysis of voltage stability in electric power systems," *Electric Power System Reserach*, vol. 9, pp. 49-62, 1985.

[6] J. Carpentier, "Voltage collapse proximity indications computed from an optimal power flow," in *Proc. of Computational Conference*, Helsinki, Finland, September 1984, pp. 671-678.

[7] T. Van Cutsem, "A comprehensive analysis of mid-term voltage stability," *IEEE Transactions on Power Systems*, vol. 10, no. 3, pp. 1173-1182, August 1995.

[8] B. H Lee and K. Y. Lee, "A study on voltage collapse mechanism in electric power systems," *IEEE Trans. Power Systems*, vol. 6, pp. 966-974, August 1991.

[9] Löf. P-A., G. Anderson, and Hill. D. J., "Voltage stability indices for stressed power systems," *IEEE Transactions on Power Systems*, vol. 8, pp. 326-335, Febrauary 1993.

[10] P-A, Löf, G. Andersson, and D. J. Hill, "Voltage dependent reactive power limits for voltage stability studies," *IEEE Transactions on Power Systems*, vol. 10, pp. 220-228, Febrauary 1995.

[11] B. Gao, G. K. Morison, and P. Kundur, "Voltage stability evaluation using modal analysis," *IEEE Transactions on Power Systems*, vol. 7, pp. 1529-1542, November 1992.

[12] J. Guckenheimer, "Towards a global theory of singularly perturbed dynamical systems," *Progress in Nonlinear Differential Equations and Their Applications*, vol. 19, pp. 214-225, 1996.

[13] H. G. Kwanty, A. K. Pasrija, and Bahar. L.Y., "Loss of steady state Stbility and voltage collapse in electric power systems," in *Proceedings of 24th conference on Decision and Control*, Ft. Lauderdale, Fl, 1985.

[14] T. Van Cutsem and C. Vournas, *Voltage stability of electric power systems*. Boston, USA: Kluwer Academic Publishers, 1998.

[15] V. Ajjarapu and C. Christy, "The continuation power flow: A tool for steady state voltage stability analysis," *IEEE Transactions on Power Systems*, vol. 7, February 1992.

[16] G. K. Morison, B. Gao, and P. Kundar, "Voltage stability analysis using static and dynamic approaches.," *IEEE Transactions on Power Systems*, vol. 8, no. 3, pp. 1159-1171, August 1993.

[17] M. M. Begovic and A. G. Phadke, "Control of voltage stability using sensitivity analysis," *IEEE Transactions on Power Systems*, vol. 7, no. 1, pp. 114-123, February 1992.

[18] C. L. DeMarco and T. J. Overbye, "Improved techniques for power systen voltage stability assessment using energy methods," *IEEE Transactions on Power Systems*, vol. 6, no. 4, pp. 1446-1452, November 1991.

[19] G. Huang and Zhu. T., "A new method to find the voltage collapse point," in *Proc. of Power Engineering Society Winter Meeting IEEE*, Edmonton, Canada, July 1999, pp. 1324-1329.

[20] J. Bian and P. Rastgoufard, "Power system voltage stability and security assesment," in *Third Biennial Symposium on Induxtrial Electric Power Applications*, New Orleans, LA, Nov 12-13, 1992, pp. 178-183.

[21] J. Bian, Modal analysis of large scale power systems voltage stability and Voltage collapse, December 1992., Ph. D. Dissertation, Tulane University.

[22] C. Sharma and G. Marcus, "Determination of Power Sytem Voltage Stability Using Modal Analysis," in *POWERENG 2007*, Portugal, April 2007.

[23] C. Li-Jun and Istavan. E., "Power system static voltage stability analysis considering all active and reactive power controls - singular value approach," in *Proc. of IEEE Power Tech*, 2007, pp. 367-373.

[24] Y. G. Zeng, A. Berizzi, and P. Marannino, "Voltage stability analysis considering dynamic load model," in *Proceedings of the 4th International Conference on Advances in Power System Control, Operation and Management, APSCOM-97*, Hong Kong, November 1997.

[25] Xu. Wison and M. Yakout, "Voltage stability analysis using generic dynamic load models," *IEEE Transactions on Power Systems*, vol. 9, no. 1, February 1994.

[26] M. H. Haque and U. M. R. Pothula, "Evaluation of Dynamic Voltage Stability of a Power System," in *POWERCON 2004*, Singapore.

[27] C. C. Liu, "Characterization of a voltage collapse mechanism due to the effect of on-load tap changers," in *1986 IEEE International Symposium on Circuits and systems*, vol. 3, May 1986, pp. 1028-1030.

[28] C. C. Liu and T. Vu. Khoi, "Analysis of Tap-Changer Dynamics and Construction of voltage Stability Regions," *IEEE Transaction on circuits and systems*, vol. 36, no. 4, April 1989.

[29] Y. Sekine and H. Ohtsuki, "Cascaded voltage collapse," *IEEE Transactions on Power Systems*, vol. 5, no. 1, pp. 250-256, February 1990.

[30] K. Sun, S. Likhate, V. Vittal, V. S. Kolluri, and S. Mandal, "An online dynamic security assessment scheme using phasor measurement and decision trees," *IEEE Transactions on Power Systems*, vol. 22, no. 4, pp. 1935-1943, November 2007.

[31] C. S. M. Wong, P. Rastgoufard, and D. Mader, "Voltage Stability Studies Using Real-Time Simulation Computing," in *40th Southeastern Symposium on System Theory, 2008. SSST 2008*, March 2008, pp. 410 – 414.

[32] "Blackout experiances and lessons, best practices for system dynamic performace, and the role of new technologies," Power and Energy Society, of the Institute of Electricle and Electronic Engineering, IEEE Task Force Report 07TP190, July 2007.

[33] A. Atputharajah and K. S. Tapan, "Power system blackouts- Literature review," in *Fourth International Conference on Industrial and Information Systems, ICIIS 2009*, Sri Lanka, December 2009, pp. 28 - 31.

[34] C. W. Lee, John. A. C., 1 C. Lawrence, R. R. Charles, and E. B. Carl, "Prevention ofpower failures. Volume 1- Report of the commission submitted to the President by Federal Power Commission," July 1967.

[35] M. Ilic et al., "Special Issue on Power Technology and Policy: Forty Years after the 1965 Blackout," *Proceedings of the IEEE*, vol. 93, no. 11, November 2005.

[36] "Blackout on August 14, 2003 Final Report February by New York Independent System Operator," Febrauary Feb 2005.

[37] L. Chunyan, S. Yuanzhang, and C. Xiangyi, "Recommendations to improve power system security: Lessons learned from the Europe blackout on Nov 4th 2006.," in *UPEC-2007*.

[38] "Arizona-Southern California outages on September 8th 2011 ," FERC and NERC,.

[39] T. Athay, V. R. Sherkat, R. Podmore, R. Virmani, and C. Puech, "Transient Energy Analysis. Final report of U.S department of energy," Prepared by systems control, Inc.,

Contract No. Ex-76-C-012076, June 1979.

[40] C. S. M. Wong, I. Leevongwat, and P. Rastgoufard, "Angle and magnitude stability using Real-Time Simulation," in *Transmission and Distribution Conference and Exposition, 2008 T&D. IEEE/PES*, April 2008, pp. 1 - 4.

[41] C. S. M. Wong, Unification of Angle and Magnitude Stability to InvestigateVoltage Stability of Large-Scale Power System. PhD thesis, Dept. ofElectrical Engineering and Computer Science, 2007, Tulane University.

[42] N. Beeravolu, Pattern Recognition of Power Systems Volatge Stability Using Real Time Simulations, 2010, M.S Thesis, University of New Orleans.

[43] R. O. Duda, P. E. Hart, and Stork. D. G., *Pattern Classification*, 2nd ed.: John Wiley & Sons,Inc., 2000.

[44] T. Poggio and S. Smale, "The mathematics of learning: Dealing with data," *Amer. Math. Soc. Notice*, vol. 50, no. 5, pp. 537-544, 2003.

[45] R. M. Rifkin, Everything Old is New Age: A fresh look at historical Approaches to Machine Learning, 2002, PhD thesis, Massachusetts Institute of Technology.

[46] Robert Tibsherani, "Rigression shrinkage and selction via the LASSO," *Journal of the Royal Statistical Society*, vol. Volume 58, no. Issue 1, pp. 267-288, 1996.

[47] S. Bernhard, H. Ralf, and S. Alex, "A generalized representar theorem," in *14th Annual conference on computational learning theory*, 2001, pp. 416-426.

[48] W. Grace, "Spline models for observational data," *CBMS-NSF Regional conference series in applied mathematics. Society for Industrial & Applied Mathematics*, vol. 59, 1990.

[49] E. E. Bernabeu, Methodology for a Security-Dependability Adaptive Protection Scheme based on Data Mining, 2009, PhD Thesis, Virginia Polytechnic Institute and State University.

[50] K.R. Padiyar, *Power System Dynamics: Stability & Control*. India: B.S. Publications, 2002.

Vita

The author was born in 1986, in India. He completed his bachelors of technology degree in Electrical and Electronics Engineering from JNTU, Hyderabad, India in 2007 with distinction. He finished his Masters and PhD in Electrical Engineering from the University of New Orleans in December 2010 and December 2013. He worked as an intern in summer 2009 at Entergy Services Inc. The author worked on several research projects for Entergy as a Research Assistant under Prof. Dr. Parviz Rastgoufard. Currently he is working as a consultant Standards Engineer for Design Basis, Entergy Services Inc through IK Power System Solutions Inc. His areas of interests are real time simulation studies, EMTP modeling, voltage stability, power system protection and relaying, and protection relay testing and commissioning.